The Plant Cell, Vol. 28: 102–129, January 2016, www.plantcell.org

Pipecolic Acid Orchestrates Plant Systemic Acquired Resistance and Defense Priming via Salicylic Acid-Dependent and -Independent Pathways

Friederike Bernsdorff,[a] Anne-Christin Döring,[a] Katrin Gruner,[a] Stefan Schuck,[a] Andrea Bräutigam,[b,c] and Jürgen Zeier[a,c,1]

[a] Institute for Molecular Ecophysiology of Plants, Department of Biology, Heinrich Heine University, D-40225 Düsseldorf, Germany
[b] Institute for Plant Biochemistry, Department of Biology, Heinrich Heine University, D-40225 Düsseldorf, Germany
[c] Cluster of Excellence on Plant Sciences (CEPLAS), Heinrich Heine University, D-40225 Düsseldorf, Germany

We investigated the relationships of the two immune-regulatory plant metabolites, salicylic acid (SA) and pipecolic acid (Pip), in the establishment of plant systemic acquired resistance (SAR), SAR-associated defense priming, and basal immunity. Using SA-deficient *sid2*, Pip-deficient *ald1*, and *sid2 ald1* plants deficient in both SA and Pip, we show that SA and Pip act both independently from each other and synergistically in *Arabidopsis thaliana* basal immunity to *Pseudomonas syringae.* Transcriptome analyses reveal that SAR establishment in Arabidopsis is characterized by a strong transcriptional response systemically induced in the foliage that prepares plants for future pathogen attack by preactivating multiple stages of defense signaling and that SA accumulation upon SAR activation leads to the downregulation of photosynthesis and attenuated jasmonate responses systemically within the plant. Whereas systemic Pip elevations are indispensable for SAR and necessary for virtually the whole transcriptional SAR response, a moderate but significant SA-independent component of SAR activation and SAR gene expression is revealed. During SAR, Pip orchestrates SA-dependent and SA-independent priming of pathogen responses in a FLAVIN-DEPENDENT-MONOOXYGENASE1 (FMO1)-dependent manner. We conclude that a Pip/FMO1 signaling module acts as an indispensable switch for the activation of SAR and associated defense priming events and that SA amplifies Pip-triggered responses to different degrees in the distal tissue of SAR-activated plants.

INTRODUCTION

In tissue inoculated by pathogenic microbes, plants are able to initiate a basal immune program that counteracts microbial infection. Plant basal resistance or pathogen-associated molecular pattern (PAMP)-triggered immunity (PTI) involves recognition of microbial structures by plant pattern recognition receptors, defense signal transduction, and transcriptional activation of defense-related gene expression (Boller and Felix, 2009). Yet, PTI can be overcome by well-adapted pathogen isolates. However, previous pathogen encounters can render plants significantly more resistant to a future challenge. For instance, systemic acquired resistance (SAR), a state of heightened resistance of the entire plant foliage to a broad spectrum of biotrophic and hemibiotrophic phytopathogens, is induced by a localized leaf inoculation with avirulent or virulent microbial pathogens (Mishina and Zeier, 2007; Fu and Dong, 2013). Plants with activated SAR exhibit enhanced systemic expression of antimicrobial PR proteins and other augmented immune responses (Sticher et al., 1997). In addition, biologically induced SAR conditions plants to react more quickly and vigorously to subsequent pathogen attack (Jung et al., 2009; Návarová et al., 2012), a phenomenon also designated as defense priming (Conrath, 2011).

The establishment of SAR is regulated by signal-active plant metabolites (Dempsey and Klessig, 2012; Shah and Zeier, 2013). From ~1980 onwards, multiple studies have provided evidence that the phenolic defense hormone salicylic acid (SA) plays a pivotal role in SAR (reviewed in Vlot et al., 2009). The pathogen-induced biosynthesis of SA in *Arabidopsis thaliana* proceeds via isochorismate synthase-mediated conversion of chorismate to isochorismate (Nawrath and Métraux, 1999; Wildermuth et al., 2001). The Arabidopsis *sid2-1* mutant, which is defective in *ISOCHORISMATE SYNTHASE1* (*ICS1*), is unable to accumulate pathogen- and stress-inducible SA and is impaired in SAR activation (Nawrath and Métraux, 1999). Although SA was previously proposed as the mobile compound that travels from inoculated to distal leaves to induce SAR (Shulaev et al., 1995; Mölders et al., 1996), genetic studies support the notion that SA is not a SAR long-distance signal but that its isochorismate-derived de novo biosynthesis in systemic leaf tissue is required for proper SAR (Vernooij et al., 1994; Attaran et al., 2009). Since then, several other candidate long-distance signals have been suggested (reviewed in Shah and Zeier, 2013). A predominant portion of SA downstream responses is dependent on the transcriptional coactivator NON-EXPRESSOR OF PATHOGENESIS-RELATED GENES1 (NPR1), which has been identified, in addition to its paralogs NPR3 and NPR4, as a bona fide SA receptor (Fu et al., 2012; Wu et al., 2012). NPR1 acts as a central regulator of SAR (Fu and Dong, 2013).

[1] Address correspondence to juergen.zeier@uni-duesseldorf.de.
The author responsible for distribution of materials integral to the findings presented in this article in accordance with the policy described in the Instructions for Authors (www.plantcell.org) is: Jürgen Zeier (juergen.zeier@uni-duesseldorf.de).
www.plantcell.org/cgi/doi/10.1105/tpc.15.00496

In addition to SA and NPR1, FLAVIN-DEPENDENT MONOOXYGENASE1 (FMO1) is a critical component of biologically induced SAR in Arabidopsis (Mishina and Zeier, 2006; Jing et al., 2011). The strongly pathogen-inducible *FMO1* gene encodes a flavin monooxygenase that is activated in both locally inoculated and distal leaves (Bartsch et al., 2006; Koch et al., 2006; Mishina and Zeier, 2006). Notably, functional FMO1 is necessary for SA accumulation in the systemic, noninoculated leaves but dispensable for SA production in inoculated tissue (Mishina and Zeier, 2006). A biochemical characteristic of distinct FMOs from plants, insects, and mammals is that they are able to oxidize amino or sulfide groups within small metabolic substrates (Schlaich, 2007). We therefore previously hypothesized that an endogenously produced plant amine, amino acid, or S-containing metabolite might play a central function in SAR (Mishina and Zeier, 2006).

This hypothesis was confirmed by identifying the non-protein amino acid pipecolic acid (Pip; homoproline) as a critical SAR regulator (Návarová et al., 2012). Alongside with SA, Pip accumulates to high amounts in Arabidopsis leaves inoculated with SAR-inducing *Pseudomonas syringae* bacteria as well as in leaves distant from initial inoculation. Very specifically, and in contrast to SA and many other accumulating metabolites, Pip is enriched in phloem exudates collected from inoculated leaves, indicating specific transport of Pip out of inoculated leaves (Návarová et al., 2012). Pipecolic acid is a plant natural product with widespread occurrence throughout the angiosperms (Morrison, 1953; Zacharius et al., 1954), and its accumulation in leaves after inoculation with bacterial, fungal, or viral pathogens has been documented for rice (*Oryza sativa*), potato (*Solanum tuberosum*), tobacco (*Nicotiana tabacum*), soybean (*Glycine max*), and Arabidopsis (Pálfi and Dézsi, 1968; Návarová et al., 2012; Vogel-Adghough et al., 2013; Aliferis et al., 2014). In addition, Pip is overproduced in Arabidopsis autophagy mutants that exhibit stress-related phenotypes (Masclaux-Daubresse et al., 2014).

Feeding studies with isotope-labeled Lys demonstrated that, like animals (Broquist, 1991), plants synthesize L-Pip from Lys (Fujioka and Sakurai, 1997) and strongly suggested that Lys-to-Pip conversion in plants involves both a classical aminotransferase reaction removing the α-amino group from Lys and a subsequent reductase activity (Gupta and Spenser, 1969; Zeier, 2013). An aminotransferase with strong substrate specificity for Lys is encoded by *AGD2-LIKE DEFENSE RESPONSE PROTEIN1* (*ALD1*) (Song et al., 2004a). Similar to *FMO1* (Mishina and Zeier, 2006), *ALD1* has been identified as an essential SAR component that is upregulated in both locally inoculated and distal leaf tissue (Song et al., 2004b). Our recent finding that *ald1* knockout mutants are not able to biosynthesize and accumulate Pip after pathogen inoculation indicates that ALD1 is the aminotransferase required for the Lys-derived biosynthesis of Pip (Návarová et al., 2012). Moreover, the SAR defect of Pip-deficient *ald1* can be rescued by exogenous supply of Pip in physiological doses, demonstrating that Pip accumulation is required for SAR activation (Návarová et al., 2012). Exogenous Pip is also sufficient to increase resistance to *P. syringae* in wild-type and *ald1* plants to a similar degree as biological SAR (Návarová et al., 2012). Notably, Pip feeding is able neither to restore the SAR defect of *fmo1* nor to increase pathogen resistance in this mutant, indicating that Pip requires functional *FMO1* to activate SAR (Návarová et al., 2012). Like for *P. syringae*-induced SAR, Pip accumulation and *FMO1* are also integral parts of the systemic immune response induced by local oviposition of insect eggs in Arabidopsis (Hilfiker et al., 2014).

The activation of SAR in noninfected distal tissue of pathogen-inoculated plants relies on the perception and amplification of endogenous plant signals (Shah and Zeier, 2013). Our current working model implies that Pip is a central player of a feedback amplification mechanism that realizes systemic SA accumulation and SAR establishment (Návarová et al., 2012; Zeier, 2013). Once established, SAR primes Arabidopsis plants for effective defense responses to future pathogen challenge. These responses include the accumulation of the phytoalexin camalexin and expression of a series of defense-related genes, including *ALD1*, *FMO1*, and *PR1.* Systemically elevated Pip during SAR is necessary and sufficient for the SAR-associated priming response (Návarová et al., 2012; Zeier, 2013).

In this study, we investigate the interplay of Pip and SA in Arabidopsis immune signaling and provide a detailed characterization of the systemic transcriptional response associated with SAR. Systemic transcriptional reprogramming upon localized *P. syringae* inoculation involves enhanced expression of microbial pattern recognition receptors, various defense signaling components, and specific transcription factor classes, as well as a massive downregulation of photosynthetic and growth-related genes. We show that Pip orchestrates SAR and virtually the whole transcriptional SAR response via SA-dependent and, less prominently, SA-independent activation pathways. Our data indicate that activation of a primed state in distal leaves of locally inoculated plants requires functional FMO1 downstream of Pip and that SAR priming of a subset of genes proceeds in SA-deficient *sid2* to a similar extent as in the wild type. Our results therefore emphasize the significance of partially SA-independent signaling events during SAR establishment and the realization of SAR-associated defense priming. Moreover, they indicate that Pip and SA act both synergistically and independently from each other to mediate *PR* gene expression and plant basal resistance to *P. syringae*.

RESULTS

The SA and Pip Defense Pathways Provide Additive Contributions to Basal Resistance

To obtain deeper insights into the interplay between the immune signals Pip and SA in mediating Arabidopsis basal resistance, SAR establishment, and defense priming, we comparatively investigated resistance responses of the Col-0 wild type, Pip-deficient *ald1* (Návarová et al., 2012), SA induction-deficient *sid2-1* (*sid2*; Nawrath and Métraux, 1999), and a *sid2 ald1* double mutant unable to generate both SA and Pip after pathogen inoculation. Whereas *ald1* represents a T-DNA knockout line for *ALD1* (Song et al., 2004b; Návarová et al., 2012), *sid2* was previously obtained by ethyl methanesulfonate mutagenesis and carries a single base pair mutation in the *ICS1* coding region that results in a premature stop codon and a full loss of *ICS1* function (Nawrath and Métraux, 1999; Wildermuth et al., 2001). The *sid2 ald1* double mutant was generated by screening progeny from a cross of the single mutants (Supplemental Figures 1 and 2).

Upon leaf inoculation with the SAR-inducing bacterial strain *Pseudomonas syringae* pv *maculicola* ES4326 (*Psm*) (Mishina and

Zeier, 2007; Attaran et al., 2009; Jing et al., 2011), we observed strong increases of *ALD1* and *ICS1* transcript levels in wild-type Col-0 plants, increases of *ICS1* but not *ALD1* in *ald1*, and elevations of *ALD1* but not *ICS1* in *sid2*. Moreover, *sid2 ald1* lacked both basal and pathogen-induced expression of *ALD1* and *ICS1* (Figure 1A). On the metabolite level, *Psm* attack triggered a strong accumulation of both Pip and SA in inoculated (1°) leaves and in distal (2°), noninoculated leaves of Col-0 plants. By contrast, *sid2 ald1* produced neither Pip nor SA after pathogen inoculation and contained only faint basal levels of the two immune-regulatory metabolites (Figures 1B and 1C). Consistent with our previous analyses (Návarová et al., 2012), *ald1* completely lacked pathogen-induced Pip accumulation but was able to activate SA production in inoculated leaves, whereas *sid2* showed a reciprocal accumulation pattern (Figures 1B and 1C).

To assess basal resistance to bacterial attack, we compared the growth of the virulent *Psm* strain in leaves of Col-0, *ald1*, *sid2*, and *sid2 ald1* 3 d after inoculation. Both *ald1* and *sid2* allowed higher bacterial multiplication than the wild type (Figure 2A), confirming

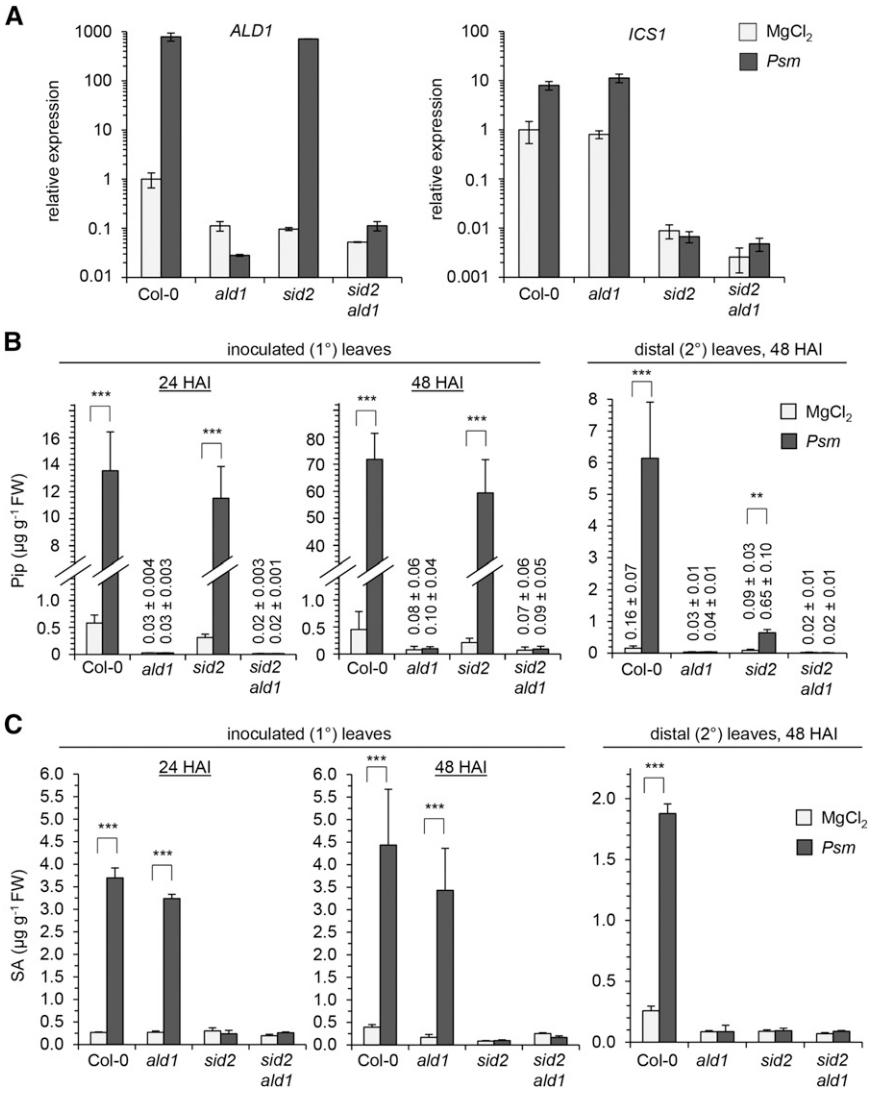

Figure 1. Pip and SA Biosynthesis in Local and Systemic Tissue of Wild-Type Col-0, *ald1*, *sid2*, and *sid2 ald1* Plants Inoculated with SAR-Inducing *Psm*.

(A) Expression of *ALD1* (left) and *ICS1* (right) in *Psm*-inoculated leaves at 24 h after inoculation (HAI). Infiltration with 10 mM $MgCl_2$ served as a mock control treatment. Transcript levels were assessed by qPCR analysis and expressed relative to the Col-0 mock control value. Data represent the mean ± SD of three biological replicate leaf samples from different plants. Each biological replicate consists of two leaves from one plant. Expression values for each biological replicate represent the mean of two technical replicates.

(B) and **(C)** Accumulation of Pip **(B)** and free SA **(C)** in *Psm*-inoculated (1°) leaves at 24 and 48 HAI (left) and in distal, noninoculated (2°) leaves (right) at 48 HAI. Data represent the mean ± SD of at least three biological replicate leaf samples from different plants. Each biological replicate consists of six leaves from two plants. Asterisks denote statistically significant differences between *Psm* and $MgCl_2$ samples (***$P < 0.001$ and **$P < 0.01$; two-tailed *t* test). Numerical values for samples with very low metabolite contents are given above the respective bars.

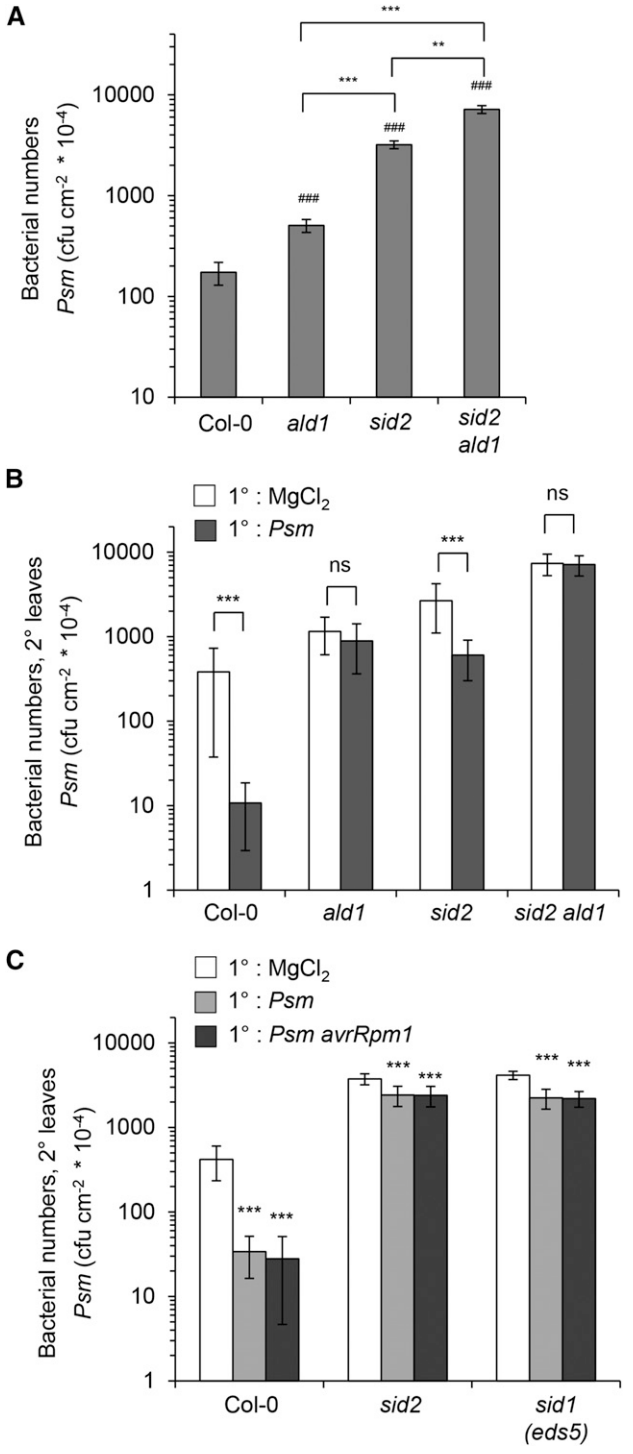

Figure 2. Analyses of Basal Resistance to *Psm* and SAR in Pip- and/or SA-Deficient Mutant Plants.

(A) Basal resistance of Col-0, *ald1*, *sid2*, and *sid2 ald1* plants to *Psm*. Three leaves per plant were inoculated with a suspension of *Psm* (OD_{600} = 0.001) and bacterial numbers quantified 3 d later. Bars represent mean values (±SD) of colony-forming units (cfu) per square centimeter from at least seven biological replicate samples (*n*) derived from different plants. Each biological replicate consists of three leaf discs harvested from different leaves of one plant. Number signs denote statistically significant differences from the Col-0 wild-type value ($^{\#}P < 0.05$, $^{\#\#}P < 0.01$, and $^{\#\#\#}P < 0.001$; two-tailed *t* test). Asterisks designate statistically significant differences between indicated samples. To test whether the effects of *ald1* and *sid2* on bacterial proliferation are additive or synergistic, a linear model was used ($\log_{10}$ bacterial count ~ *ald1*sid2*). No significant interaction of *ald1*sid2* was detected both according to the F-test and according to Akaikes information criterion (P = 0.0508, $AIC_{synergistic} = -120$ $AIC_{additive} = -122.7$); hence, the effect is additive.

(B) SAR assay with Col-0, *ald1*, *sid2*, and *sid2 ald1* plants. Lower (1°) leaves were infiltrated with either 10 mM $MgCl_2$ or *Psm* (OD_{600} = 0.005) to induce SAR, and 2 d later, three upper leaves (2°) were challenge-infected with *Psm* (OD_{600} = 0.001). Bacterial growth in upper leaves was assessed 3 d after 2° leaf inoculation ($n \geq 7$; as described in **[A]**). Asterisks denote statistically significant differences between *Psm* pretreated and mock control samples (***P < 0.001; ns, not significant, two-tailed *t* test).

(C) Biological SAR induction upon 1° leaf inoculation with compatible *Psm* and incompatible *Psm avrRpm1* in Col-0, *sid2*, and *sid1* plants ($n \geq 7$; as described in **[A]** and **[B]**). Asterisks denote statistically significant differences between *Psm* or *Psm avrRpm1* (OD_{600} = 0.005) pretreated and mock control samples (***P < 0.001; two-tailed *t* test).

the previously suggested requirements for Pip and SA in the full basal immunity program at inoculation sites (Nawrath and Métraux, 1999; Návarová et al., 2012). The *sid2* mutant permitted significantly higher bacterial multiplication than *ald1*, indicating that the relative contribution of SA to basal resistance is higher than that of Pip. Notably, leaf-inoculated *sid2 ald1* showed the weakest resistance phenotype of all investigated lines and allowed a significantly higher bacterial multiplication than Col-0, *ald1*, and *sid2* (Figure 2A). This indicates that SA and Pip provide additive contributions to Arabidopsis basal immunity against *P. syringae*.

Pip Regulates SAR via SA-Dependent and -Independent Activation Pathways

The 2° leaves of locally inoculated *sid2* plants accumulated Pip to a moderate but significant extent, suggesting that pathogen-triggered systemic responses are not fully suppressed in *sid2* (Figure 1B). On the contrary, *ald1* was unable to elevate SA in 2° leaves, corroborating our previous results showing the necessity of Pip for the activation of SA biosynthesis and concomitant SA accumulation in distal leaves (Figure 1C; Návarová et al., 2012). To directly examine the SAR response in the lines under investigation, we inoculated plants with *Psm* in lower, 1° leaves to induce SAR or performed mock treatments with 10 mM $MgCl_2$ to generate appropriate noninduced control plants and then challenge-inoculated upper, 2° leaves of both pathogen-inoculated and mock-treated plants with *Psm* 2 d after the primary treatment. Bacterial growth in upper leaves was assessed another 3 d later (Mishina and Zeier, 2007; Attaran et al., 2009; Jing et al., 2011; Návarová et al., 2012). In these assays, wild-type Col-0 plants exhibited a strong SAR response and the bacterial multiplication in challenge-infected leaves was generally attenuated by 95 to 98% as a consequence of SAR induction (Figure 2B). The Pip-deficient *ald1* mutant was not able to activate any SAR upon

attempted induction (Song et al., 2004b; Návarová et al., 2012), confirming the previously reported necessity of Pip accumulation in SAR establishment (Návarová et al., 2012). Remarkably, the SA-deficient *sid2* mutant was able to significantly induce resistance upon localized *Psm* inoculation in distal leaves (Figure 2B). Although the observed SAR response in *sid2* was small compared with wild-type SAR (a 50 to 80% reduction of bacterial growth), the effect was reproducible between experiments and occurred, besides in *sid2*, in *sid1* (Figure 2C), another Arabidopsis mutant unable to activate stress-induced SA biosynthesis (Nawrath and Métraux, 1999), and in an *ics1 ics2* double mutant (Supplemental Figure 3), which is not only blocked in induced SA production but also exhibits strongly diminished basal SA levels (Garcion et al., 2008). Moreover, the hypersensitive response-inducing *Psm avrRpm1* strain triggered partial SAR activation in *sid2* in a similar manner than the compatible *Psm* strain (Figure 2C). These results show that a moderate SAR response in plants can be triggered independently of inducible SA biosynthesis but not independently of Pip biosynthesis. However, SA accumulation upon pathogen encounter is required to realize a full SAR response. The residual, SA-independent SAR effect is absent in the *sid2 ald1* double mutant, indicating that activation of this pathway and of the predominant, SA-dependent SAR pathway do both require Pip (Figure 2B). In sum, these data strongly suggest that Pip is a central regulatory metabolite for SAR that controls both SA-dependent and -independent SAR activation pathways.

Transcriptional Reprogramming in Distal Leaves of SAR-Activated Plants: Increased Readiness for Pathogen Defense Coupled with Decreased Photosynthesis, General Metabolism, and Growth

SAR establishment following 1° leaf inoculation involves increased expression of a whole battery of defense-related genes in the distal leaves (Ward et al., 1991; Gruner et al., 2013). To assess the contribution of Pip and SA to SAR on the transcriptional level, the transcriptional SAR response of Col-0 was characterized at the whole-genome level and compared with the responses in *sid2* and *ald1*. Compatible *Psm* or hypersensitive response-inducing *Psm avrRpm1* trigger SAR in Col-0 plants between days 1 and 2, and the full resistance response is apparent at 2 d after inoculation (Mishina et al., 2008; Návarová et al., 2012). We thus determined the transcriptional changes that occur in 2° leaves 2 d after *Psm* treatment of 1° leaves compared with 1° mock treatment by Illumina TruSeq RNA sequencing analyses. A first experimental set consisted of three independent, replicate SAR experiments (experiments 1 to 3) with Col-0 and *sid2* plants, and a second analogous set involved Col-0 and *ald1* (experiments 4 to 6). Principle component analysis (PCA) identified *Psm* treatment variation as the major variable between the samples, accounting for 58.0% of the variation. The second variable was experiment variation between the first and second experimental sets and accounted for 15.7% of the variation, indicating that experimental variation was small compared with treatment variation. To be conservative, the six Col-0 replicates were combined for analysis. The PCA also showed that in Col-0, the distance between mock and *Psm* treatment samples was widest. The distance between *sid2* samples was small and the distance between *ald1* samples was virtually nonexistent (Supplemental Figure 4).

A threshold cutoff of expression values (reads per million) was defined that excluded genes with very low expression levels from the RNA-seq data set, i.e., genes that did not reach expression values of at least 5 in any of the mock or *Psm* samples. This reduced the set of 28,496 totally RNA-seq covered genes to a set of 15,239 expressed genes. To determine statistically significant changes in gene expression of *Psm* versus mock treatments for Col-0, *sid2*, and *ald1*, a false discovery rate (FDR) of 0.01 was assumed (Benjamini and Hochberg, 1995). Among the 15,239 investigated genes, 3413 were upregulated (designated as SAR^+ genes) and 2893 were downregulated (SAR^- genes) in a statistically significant manner in the Col-0 wild type (Figure 3A; Supplemental Data Set 1). To quantitatively assess the transcriptional changes between the SAR-induced and mock control state, we calculated $\log_2$-transformed ratios of the mean of expression values for *Psm* and mock samples (*P*/M-fold changes). The $\log_2$ *P*/M-fold changes for Col-0 averaged over all the SAR^+ and SAR^- genes were 2.05 and −1.57, respectively (Figure 3B).

To identify and illustrate physiological and metabolic processes altered in Col-0 plants upon SAR establishment, we tested whether the up- and downregulated SAR genes are enriched in MapMan bins or particular Arabidopsis gene families (Thimm et al., 2004; http://www.arabidopsis.org/). Strikingly, 86% of the investigated genes annotated for an involvement in photosynthesis were significantly downregulated upon SAR induction in Col-0 (Figure 4A). Similarly, genes belonging to the MapMan categories photosynthetic light reactions, Calvin cycle, photorespiration, and tetrapyrrole biosynthesis were predominantly downregulated (Figure 4A, Supplemental Figures 5 to 7). Moreover, genes involved in starch metabolism and genes of the category major CHO metabolism were strongly overrepresented in the SAR^- gene group (Figures 4A and 4B). To a lesser extent, this was also valid for genes of the categories lipid metabolism, amino acid metabolism, and secondary metabolism (Figure 4B). In addition, genes of the MapMan category cell wall were enriched among SAR^- genes (Figure 4B). A closer look at the family level revealed that many genes coding for proteins involved in cell wall modification and growth (fasciclin-like arabinogalactan proteins, expansins, and xyloglucan endotransglucosylase/hydrolases) as well as genes associated with wax and cutin biosynthesis were strongly downregulated during SAR (Figure 4C). This suggests that in the distal leaves of SAR-activated plants, photosynthesis, several primary and secondary metabolic pathways, and growth processes are reduced compared with respective leaves of control plants. Gene Ontology (GO) term enrichment analysis confirmed the reduction in growth-related processes (Supplemental Data Set 2).

The massive downregulation of photosynthesis-associated genes upon SAR induction in Col-0 prompted us to comparatively investigate the photosynthetic rates of 2° leaves of plants infiltrated in 1° leaves 2 d earlier with *Psm* or mock solution. We measured the CO_2 uptake of individual leaves using infrared gas analysis (IRGA) to determine the maximum rates of photosynthetic carbon assimilation (von Caemmerer and Farquhar, 1981). Upon SAR induction in Col-0, the rate of CO_2 uptake of 2° leaves significantly dropped from ~8 to 4 μmol m^{-2} s^{-1}, indicating a marked

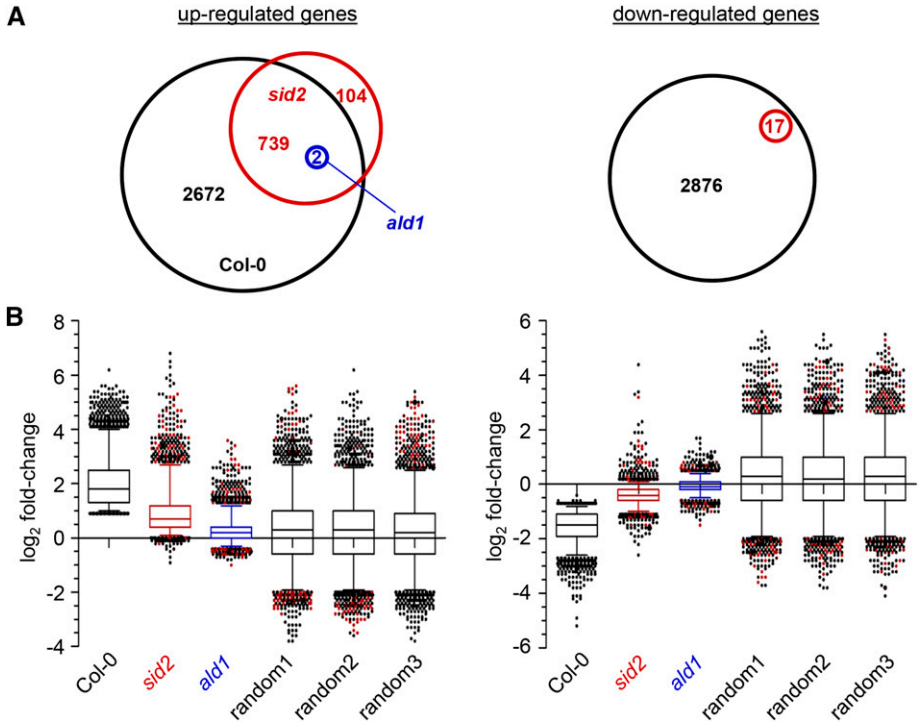

Figure 3. Transcriptional SAR Response in Distal Leaves of Plants Inoculated in Primary Leaves with *Psm* (OD_{600} = 0.005) at 48 HAI.

Six independent SAR assays for Col-0 and three independent SAR experiments for both *sid2* and *ald1* were performed. Gene expression was analyzed by RNA-seq analyses of the resulting replicate samples for *Psm* and mock treatments at the whole-genome level.

(A) Venn diagram depicting numbers of differentially regulated genes between *Psm* and mock treatments of Col-0 (black), *sid2* (red), and *ald1* (blue) (FDR < 0.01). Overlap of genes is indicated. Left: significantly upregulated genes (the Col-0 genes correspond to the SAR^+ genes). Right: significantly downregulated genes (the Col-0 genes correspond to the SAR^- genes). Note that only two genes are differentially regulated in *ald1*.

(B) Distribution of *P*/M-fold changes of SAR genes in Col-0, *sid2*, and *ald1*. Box plots depict $\log_2$-transformed *P*/M-fold changes. The distribution of $\log_2$ *P*/M-fold changes for three sets of randomly selected genes (left, 3413 genes; right, 2893 genes) is included (random a, b, and c). Left, SAR^+ genes; right, SAR^- genes.

decrease in photosynthetic rates (Figure 5A). Our data thus reveal an attenuation of photosynthesis in the noninoculated distal leaves of SAR-induced wild-type plants both at the transcriptional and the physiological level. Infrared gas analysis also showed decreased water loss from 2° leaves of SAR-induced Col-0 plants, suggesting a significant decline of leaf transpiration when SAR is established (Figure 5B). Decreased stomatal apertures may thus account for the attenuation of photosynthesis in SAR-induced plants.

Analyses of the transcriptional SAR response also revealed that the categories biotic stress and signaling were overrepresented among the SAR^+ genes (Figure 4D). GO term enrichment analysis of the SAR^+ genes specified the biotic stress and signaling categories by identifying regulation of the hypersensitive response, SAR, and SA signaling and their respective parent terms as enriched processes. In addition, N-terminal protein myristoylation, Golgi-based protein targeting to membranes, and the endoplasmic reticulum unfolded protein response as well as their respective parent terms were enriched (Supplemental Data Set 3). Moreover, gene families typically involved in the perception of pathogen-derived elicitors, i.e., genes coding for nucleotide binding site (NBS)-containing resistance proteins (Tan et al., 2007), receptor-like protein kinases (RLKs; Shiu and Bleecker, 2001), and receptor-like proteins (Fritz-Laylin et al., 2005) were markedly enriched in the SAR^+ gene group (Figure 4E). Notably, a preferential accumulation of members representing specific subfamilies of the large RLK family in the SAR^+ group was apparent. For example, ~70% of cysteine-rich protein kinases in the investigated gene set were consistently upregulated upon SAR induction (Supplemental Figure 8A). In addition, defense signaling components such as mitogen-activated protein kinase kinases, calcium-dependent protein kinases, EF-hand containing proteins, and calmodulin binding proteins were overrepresented among the SAR^+ genes (Figures 4F and 4G). Among transcription factor families, a strong overrepresentation of WRKY- and NAC-type transcription factor genes was observed in the SAR^+ gene group, whereas genes for transcription factor types such as MYB, bHLH, or bZIP were not enriched (Figure 4H). Finally, compared with other major types of enzyme classes, a prominent overrepresentation of glutathione *S*-transferases among the SAR^+ genes was discernable (Figure 4I). Other, less prominent gene classes that were strongly overrepresented in the SAR^+ group involved senescence-associated genes as well as genes coding for stomatin/prohibitin/flotillin/HflK/C (SPFH) domain-containing, FAD berberine-type,

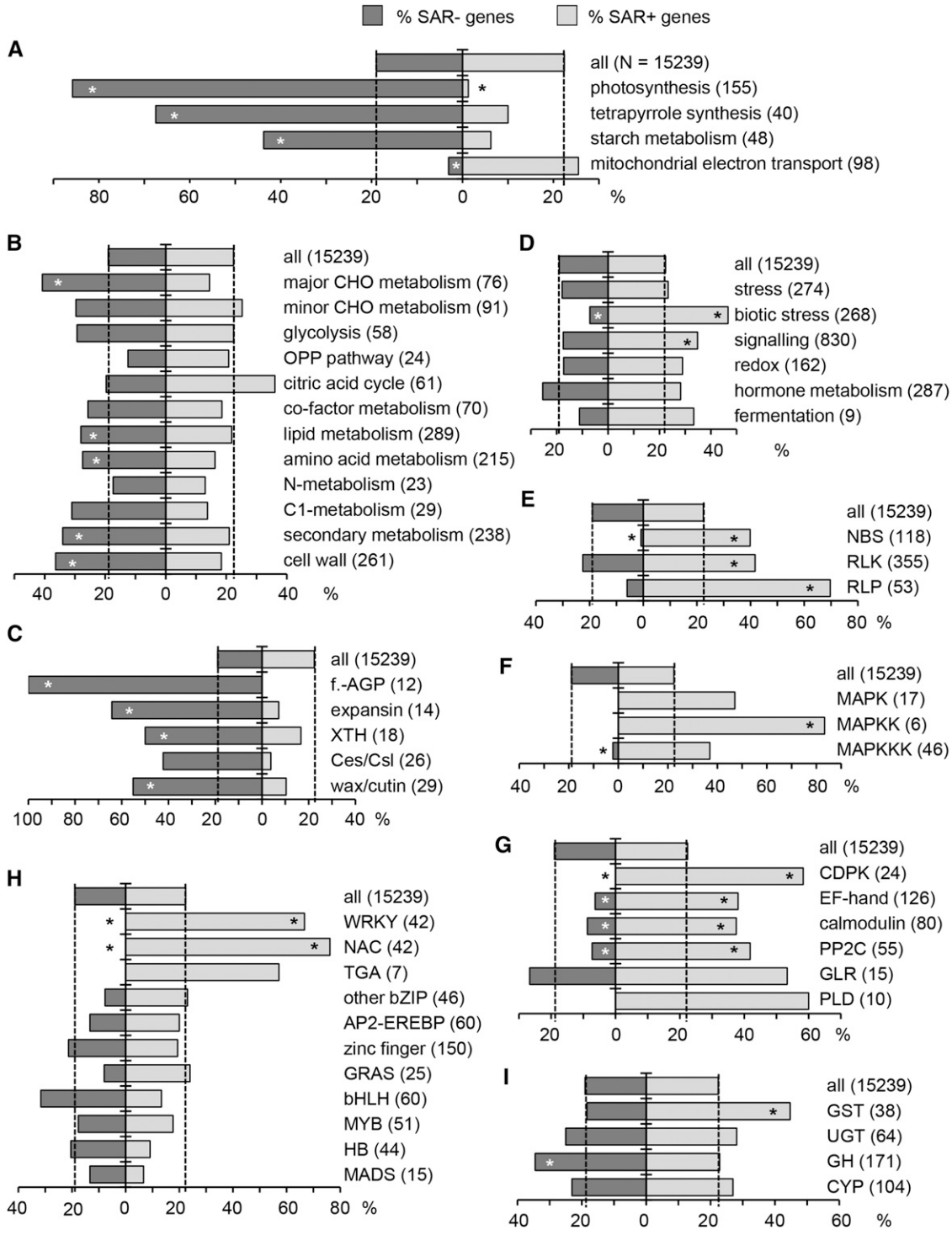

Figure 4. Percentage of SAR$^+$ and SAR$^-$ Genes in Defined Gene Groups Representing MapMan Metabolic Pathways, Functional Categories, or Arabidopsis Gene Families (http://www.arabidopsis.org).

Dashed vertical lines illustrate the percentage of SAR$^+$ and SAR$^-$ genes in the whole, RNA-seq-covered transcriptome (28,496 genes) after threshold cutoff (15,239 genes). The number of genes in each category is given in parentheses. Asterisks on the bars indicate significant enrichment or depletion of gene categories in SAR$^+$ (right) and SAR$^-$ (left) genes (Fisher's exact test, $P < 0.01$).

(A), **(B)**, and **(D)** MapMan metabolic pathways and functional categories.

VQ motif-containing proteins, and plant U-box proteins (Supplemental Figure 8B). By contrast, the general expression patterns of genes from MapMan categories such as development, cell, transport, monolignol biosynthesis, or class III peroxidase genes were hardly or not at all changed upon SAR induction (Supplemental Figure 8C).

Overall, these characteristics suggest that SAR-activated plants prepare themselves for future pathogen attack by upregulating genes involved at different stages of defense signaling, such as elicitor perception, signal transduction, and transcriptional gene activation, and by downregulating photosynthesis and growth-associated processes.

The Transcriptional SAR Response Involves a Subset of Genes Whose Systemic Expression Is Partially SA Independent

The transcriptional SAR response in the mutants was compared qualitatively and quantitatively to the wild-type response (Figure 3). According to the statistical RNA-seq analysis, the transcript levels of 2672 out of the 3413 genes that were systemically upregulated in the Col-0 wild type following SAR induction were not elevated in *sid2* in a statistically significant manner (Figure 3A). Therefore, a predominant part of the transcriptional SAR response is SA dependent. We created a list of all the SAR$^+$ genes from this group and sorted them according to their mean *P*/M-fold change in *sid2* in ascending order. Table 1 depicts the top 15 SAR$^+$ genes from this list. Among the tightly SA-regulated SAR$^+$ genes are *PATHOGENESIS-RELATED GENE1* (*PR1*), a classical marker gene for an activated SA signaling pathway and SAR (Sticher et al., 1997), *ACIREDUCTONE DIOXYGENASE3* (*ARD3*), and *GLUTAREDOXIN13* (*GRXS13*).

The quantitative RNA-seq assessment indicated that the median $\log_2$ *P*/M-fold change over all the SAR$^+$ genes for *sid2* accounted for 0.95 (Figure 3B). Although lower than the respective Col-0 value of 2.05, this value was markedly higher than the values calculated from different sets of randomly chosen genes from the total Arabidopsis genome (0.23 to 0.28). Therefore, *sid2* exhibits an attenuated but still detectable transcriptional response to *Psm* in tissue distal from inoculation. Qualitatively, 845 genes were significantly upregulated in 2° leaves of *sid2* upon 1° leaf inoculation, and 741 of them were induced in a significant manner also in the Col-0 wild type (Figure 3A). We sorted the SAR$^+$ genes within this group according to their mean *P*/M-fold change values in *sid2* in descending order. Table 2 lists 15 prominently expressed genes with strong upregulation in *sid2*.

A common feature of these genes is that their *P*/M-fold changes (their inducibility) in *sid2* are similar or even higher than in the wild type, but that their absolute expression in 2° tissue of mock- and pathogen-treated *sid2* plants is markedly lower than in Col-0. This indicates that SA amplifies their expression under both inducing and basal conditions (Table 2; Supplemental Data Set 1 and Supplemental Figure 4), and we have therefore designated these genes as partially SA independent. Strikingly, *ALD1* and *FMO1* rank among the most strongly induced genes in the systemic tissue of *sid2*, demonstrating that the transcriptional activation of Pip biosynthesis and downstream signaling can be activated during SAR in a manner that is partially SA independent. Other paradigm examples of SAR$^+$ genes that can be strongly upregulated in the absence of elevated SA are *TYROSINE AMINOTRANSFERASE3* (*TAT3*), *GLUTATHIONE S-TRANSFERASE22* (*GST22*), *PHYTOALEXIN-DEFICIENT3* (*PAD3*), and *SENESCENCE-ASSOCIATED GENE13* (*SAG13*) (Table 2). For the top members of the gene list, the high inducibility in *sid2* resulted in expression values for *Psm*-treated *sid2* samples that markedly exceeded those of mock-treated Col-0. Genes from the middle or bottom part of the gene list, however, generally showed a lower inducibility in *sid2* than in Col-0, and the values from *Psm*-inoculated *sid2* only moderately exceeded the Col-0 mock values (e.g., *PR5*, *AAC3*, and *P4H5*) or even stayed below (e.g., *FRK1*) (Table 2). Therefore, the absolute expression of the genes from the bottom part of the gene list such as *FRK1* still very much depends on SA, although a slight (but statistically significant) upregulation exists in *sid2*.

Together, these expression analyses indicate that the extent of systemic upregulation for virtually all SAR$^+$ genes is positively regulated by SA. For the majority of genes, this SA-mediated amplification is essential for a significant upregulation (SA-dependent SAR$^+$ genes; Table 1) or a noticeable induction well above basal wild-type levels (bottom part of list of partly SA-independent genes, as exemplified by *FRK1* in Table 2). However, the dependency on SA is lower for several hundred SAR$^+$ genes, which therefore exhibit a marked systemic upregulation in *sid2* (major part of the 741 partly SA-independent genes, as exemplified by the top 15 genes of Table 2). Notably, the SAR regulatory and pipecolic acid pathway genes *ALD1* and *FMO1* belong to the

Figure 4. (continued).

(C) Gene families involved in cell wall remodeling and wax/cutin biosynthesis. f.-AGP, fasciclin-like arabinogalactan proteins; XTH, xyloglucan endotransglucosylase/hydrolases; Ces/Csl, cellulose synthase/cellulose synthase-like.

(E) Gene families involved in the perception of microbial structures and early defense signal transduction. NBS, nucleotide binding site-containing resistance proteins; RLP, receptor-like proteins.

(F) MAPK cascade members. MAPKK, MAPK kinase; MAPKKK, MAPK kinase kinase.

(G) Other gene categories involved in defense signaling. CDPK, calcium-dependent protein kinases; EF-hand, EF-hand-containing proteins; calmodulin, calmodulin binding proteins; GLR, glutamate receptor-like family; PLD, phospholipase D family.

(H) Main transcription factor families. WRKY, WRKY domain family; NAC, NAM-ATAF1,2-CUC2 transcription factors; TGA, TGACG motif binding factor; bZIP, basic leucine zipper; AP2-EREBP, APETALA2 and ethylene-responsive element binding proteins; zinc finger, zinc finger superfamily; GRAS, GRAS family; bHLH, basic helix-loop-helix; MYB, MYB family; HB, homeobox-leucine zipper; MADS, MADS box.

(I) Genes for different enzyme classes. GST, glutathione *S*-transferases; UGT, UDP-dependent glycosyltransferases; GH, glycosyl hydrolases; CYP, cytochrome P450 superfamily.

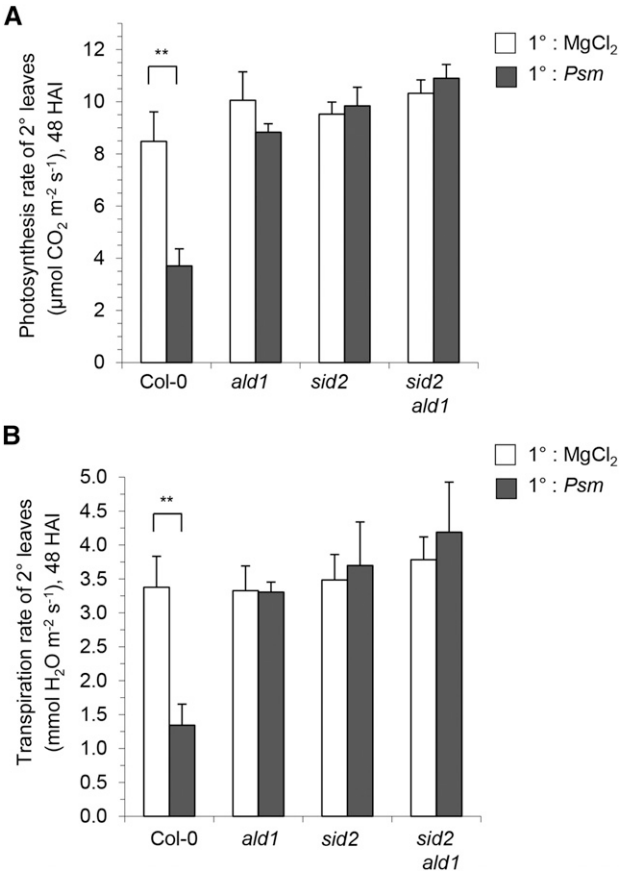

Figure 5. Photosynthesis and Transpiration Rates in 2° Leaves of 1° Leaf-Inoculated Col-0, *ald1*, *sid2*, and *sid2 ald1* Plants.

(A) CO_2 uptake rates as a measure of photosynthetic capacity at 48 h after *Psm* inoculation or $MgCl_2$ infiltration measured in distal, untreated leaves of Col-0, *sid2*, *ald1*, and *sid2 ald1* plants, as determined by IRGA. Data represent the mean ± SD of four biological replicates (CO_2 uptake rate of four distal leaves from different plants).

(B) Rates of transpiration (water loss) in distal leaves, determined as described above by IRGA.

Asterisks denote statistically significant differences between *Psm*-treated and mock control plants (**P < 0.01; two-tailed *t* test).

SAR+ genes with a pronounced SA-independent component of induction.

An Activated SA Pathway upon SAR Induction Suppresses Systemic Jasmonate Responses

The RNA-seq results show that 104 of the 845 genes systemically induced in *sid2* were not upregulated or even significantly downregulated in Col-0 upon SAR activation (Figure 3A). We listed these genes according to their Col-0 mean *P*/M-fold change values in ascending order, and Table 3 exemplifies 15 of these specifically *sid2* upregulated genes. Several jasmonate-responsive genes such as *VEGETATIVE STORAGE PROTEIN2* (*VSP2*) or *BENZOIC ACID/SALICYLIC ACID METHYLTRANSFERASE1* (*BSMT1*) belong to this group. We therefore tested whether this gene category would be actually enriched in jasmonic acid (JA)-responsive genes. A list of JA-responsive genes was taken from microarray data of Goda et al. (2008), studying the response of Arabidopsis to methyl jasmonate treatment. According to this list, the examined group of 15,239 Arabidopsis genes contained 3.2% of JA-responsive genes, and the genes systemically upregulated in Col-0 (SAR+ genes) showed a similar percentage of JA-regulated genes (3.7%; Table 4). By comparison, 12.8% of the genes systemically upregulated in *sid2* were JA responsive, and the subgroup thereof containing only genes that were not upregulated in Col-0 showed by far the highest enrichment (48.1% JA-responsive genes). These findings show that a 1° leaf inoculation with *Psm* triggers a significantly higher expression of JA-responsive genes in 2° leaves of *sid2* plants compared with Col-0 plants and indicate that an activated SA pathway in the SAR-induced wild type suppresses pathogen-inducible JA responses in systemic tissue.

Pipecolic Acid Is a Central Regulator of the Systemic Transcriptional Reprogramming Response Associated with SAR

Col-0 plants responded to the 1° *Psm* inoculation with the upregulation of 3413 and the downregulation of 2893 genes in 2° leaves. Strikingly, for the Pip-deficient *ald1* plants, only two genes, *CYSTEINE-RICH RECEPTOR-LIKE PROTEIN KINASE6* (*CRK6*) and *PLANT CADMIUM RESISTANCE1* (*PCR1*), were systemically upregulated in a statistically significant manner, and not a single gene was significantly downregulated (Figure 3A, Table 5). Moreover, albeit the statistical analyses identified *CRK6* and *PCR1* as upregulated in *ald1*, their absolute expression levels after *Psm* treatment were low and did not even exceed the values of the Col-0 mock control samples (Table 5). Therefore, the strong transcriptional reprogramming observed in 2° leaves of Col-0 plants after 1° leaf inoculation is essentially absent in *ald1*. This indicates that the accumulation of Pip upon pathogen inoculation is necessary for virtually the entire transcriptional SAR response. This also becomes evident when the MapMan heat maps of central metabolism for Col-0 and *ald1* upon (attempted) SAR induction are compared (Supplemental Figures 5 and 7). Moreover, the mean *P*/M-fold change averaged over all the SAR+ genes for *ald1* accounted for a value of 0.28, which was low compared with the Col-0 (2.05) or *sid2* (0.95) values and in the range of the values for groups of randomly chosen genes (Figure 3B).

The PCA showed that the transcriptome differences between the mock samples of Col-0 and those of *ald1* were lower than the differences of mock values between Col-0 and *sid2* (Supplemental Figure 4). This might indicate, as deduced before from the bacterial growth data (Figure 2A), that the contribution of Pip to basal resistance against *P. syringae* is lower than the contribution of SA. In addition, the SAR-associated downregulation of genes was not only blocked in *ald1* but also severely compromised in *sid2* (Figures 3A and 3B; Supplemental Figures 5 to 7). The RNA-seq results indicate that only 17 genes were significantly downregulated in *sid2*, whereas 2893 genes were repressed in Col-0 (Figure 3A). Therefore, a lack of induction of SA biosynthesis in plants seems to affect the pathogen-induced systemic gene repression to a broader extent than gene activation. Since the

Table 1. SAR$^+$ Genes Tightly Regulated by SA (SA-Dependent SAR$^+$ Genes)

			Mean Expression Value				Fold Change (Log_2)		P Value Log_2 (*P*/M)
AGI Code	Name	Gene Name/Description	Col-0 M	Col-0 *P*	*sid2* M	*sid2 P*	Col-0 *P*/M	*sid2 P*/M	*Col-0* versus *sid2*
At2g26400	*ARD3*	*ACIREDUCTONE DIOXYGENASE3*	17.5	1395.8	2.2	2.7	6.2*	0.2	0.0115#
At2g14620	*XTH10*	Xyloglucan endotransglucosylase/hydrolase 10	3.1	156.4	0.9	1.6	5.3*	0.4	0.0125#
At2g14610	*PR1*	*PATHOGENESIS-RELATED PROTEIN1*	98.7	3801.4	6.0	10.3	5.3*	0.7	0.0243#
At3g22910	*ACA13*	Putative calcium-transporting ATPase 13	5.6	247.0	1.6	3.1	5.2*	0.6	0.0160#
At3g28510	–	AAA-type ATPase family protein	11.0	411.5	1.8	2.7	5.1*	0.4	0.0271#
At3g13950	–	Unknown protein	5.4	173.3	5.3	18.6	4.8*	1.6	0.0357#
At4g10860	–	Unknown protein	1.6	57.2	0.1	0.3	4.5*	0.2	0.0634
At3g53150	*UGT73D1*	*UDP-GLUCOSYLTRANSFERASE 73D1*	1.4	49.9	0.1	0.6	4.4*	0.6	0.1793
At4g35180	*LHT7*	*LYS/HIS TRANSPORTER7*	4.2	105.9	0.7	1.9	4.4*	0.7	0.0959
At1g03850	*GRXS13*	*GLUTAREDOXIN13*	7.8	175.8	2.7	5.2	4.4*	0.7	0.0138#
At4g01870	–	TolB protein-related	8.6	196.5	3.5	17.2	4.4*	2.0	0.0716
At1g65610	*GH9A2*	*GLYCOSYL HYDROLASE 9A2*	1.6	51.6	0.6	2.2	4.4*	1.0	0.0274#
At3g61190	*BAP1*	*BON ASSOCIATION PROTEIN1*	2.1	58.6	1.2	5.8	4.2*	1.6	0.1060
At4g37530	*PER51*	Peroxidase superfamily protein	12.4	241.7	8.0	20.6	4.2*	1.3	0.0132#
At5g18270	*ANAC087*	*NAC DOMAIN CONTAINING PROTEIN87*	0.8	31.3	0.3	1.3	4.2*	0.8	0.0191#

RNA-seq analyses identified 2672 SAR$^+$ genes with significant *Psm*-induced upregulation in the Col-0 wild type and no significant induction in *sid2*. RNA samples originate from distal leaves of *Psm* (*P*)-inoculated and mock (M)-treated Col-0 and *sid2* plants at 48 HAI. Mean log_2-transformed *P*/M ratios (fold changes) are depicted, and asterisks indicate significant changes between *Psm* and mock treatments (FDR < 0.01). The 2672 genes are listed in ascending order according to their *sid2 P*/M ratios. The top 15 SAR$^+$ genes from this category (i.e., those with highest *P*/M-fold changes in Col-0) are shown. P values for differences in log_2 fold changes in Col-0 and *sid2*, determined using a linear model framework [lm(log_2(rpm) ~ genotype*treatment)], are given. Number signs indicate significant differences (P < 0.05).

systemic downregulation of photosynthetic genes is one hallmark of the transcriptional SAR response in the wild type (Figure 4A), we expected that the observed induced systemic attenuation of photosynthetic rates in Col-0 would be severely affected in *ald1* and *sid2*. IRGA analyses confirmed this assumption, since 1° leaf inoculation changed neither the photosynthetic rates nor the stomatal conductance in *ald1*, *sid2*, or *sid2 ald1*, indicating that both Pip and SA are required to mediate these responses (Figures 5A and 5B).

Pipecolic Acid Orchestrates SA-Dependent and -Independent Priming Responses upon SAR Activation

We have previously shown that the induction of SAR conditions Arabidopsis for timely and effective defense gene activation, SA biosynthesis, and camalexin accumulation. This state of defense priming becomes apparent upon a challenge infection of previously uninfected 2° leaves. Pip is a critical mediator of this SAR-associated priming response, because Pip-deficient *ald1* plants completely lack this phenomenon. Moreover, exogenously applied Pip is sufficient to promote both Col-0 and *ald1* plants into a primed, SAR-like state (Návarová et al., 2012). To investigate a possible interplay between Pip and SA in the activation of SAR-associated defense conditioning, we directly compared the abilities of Col-0, *ald1*, *sid2*, and *sid2 ald1* plants to realize biologically induced defense priming.

For this purpose, the plants were infiltrated with *Psm* or mock solution in their lower (1°) leaves, and 2 d later, the distal (2°) leaves were challenged with *Psm* or mock-infiltrated obtaining four combinations: (1°/2°) mock/mock, *Psm*/mock, mock/*Psm*, and *Psm*/*Psm* (Supplemental Figure 9A). The magnitude of defense in the challenged 2° leaves was determined for the four combinations at 10 h after inoculation (Návarová et al., 2012). We defined a particular defense response as primed if the differences between the responses of SAR-induced plants to 2° *Psm* and 2° mock treatments (*Psm*/*Psm* – *Psm*/mock), respectively, were significantly larger than the same differences in noninduced plants (mock/*Psm* – mock/mock) (Supplemental Figure 9B). Moreover, to estimate quantitative differences in the strength of priming between genotypes with activated priming, we calculated the prgain (response gain due to priming) value (see Supplemental Figure 9C for details).

We first monitored the expression of *ALD1*, *FMO1*, and *SAG13* (partially SA-independent SAR$^+$ genes; Table 2) and of *GRXS13*, *ARD3*, and *PR1* (SA-dependent SAR$^+$ genes; Table 1) as defense outputs of the SAR priming assay. SAR induction significantly primed Col-0 wild-type plants for enhanced expression of all these genes (Figure 6A; Supplemental Figure 10A). This conditioning of gene expression was completely absent in both *ald1* and *sid2 ald1* for all the examined genes (Figure 6A; Supplemental Figure 10A), corroborating the previously identified central role for Pip in the activation of SAR-associated defense priming (Návarová et al., 2012). For *sid2* plants, by contrast, the outcome of the priming assay depended on the nature of the investigated response. *FMO1* and *ALD1* expression were primed in *sid2* to a higher or similar extent, respectively, than in Col-0. The expression of *SAG13* was also significantly primed in *sid2*, but this response was markedly lower than in Col-0. Moreover, only a weak priming effect

Table 2. Partially SA-Independent SAR$^+$ Genes

				Mean Expression Value				Fold Change (Log_2)		P Value Log_2 (P/M)
Pos.	AGI Code	Name	Gene Name/Description	Col-0 M	Col-0 *P*	*sid2* M	*sid2 P*	Col-0 *P*/M	*sid2 P*/M	Col-0 versus *sid2*
1	At2g24850	*TAT3*	*TYROSINE AMINOTRANSFERASE3*	55.6	2089.5	11.1	1302.5	5.2*	6.8*	0.8032
3	At2g13810	*ALD1*	*AGD2-LIKE DEFENSE RESPONSE PROTEIN1*	12.1	378.6	0.8	140.2	4.9*	6.3*	0.1956
4	At1g19250	*FMO1*	*FLAVIN-DEPENDENT MONOOXYGENASE1*	3.9	173.2	0.4	84.3	5.2*	6.0*	0.6120
5	At2g43570	*CHI*	Putative chitinase	45.7	1523.2	3.7	286.4	5.2*	5.9*	0.7260
6	At2g29460	*GST22*	*GLUTATHIONE S-TRANSFERASE22*	5.4	274.4	1.1	112.2	5.6*	5.8*	0.9231
7	At3g09940	*MDAR3*	*MONODEHYDROASCORBATE REDUCTASE3*	4.9	126.6	0.8	93.8	4.8*	5.7*	0.8622
9	At1g02930	*GSTF6*	*GLUTATHIONE S-TRANSFERASE6*	115.7	2530.5	14.7	596.6	4.1*	5.3*	0.4248
10	At1g33960	*AIG1*	*AVRRPT2-INDUCED GENE1*	54.1	2285.9	7.6	325.5	5.4*	5.3*	0.7475
11	At3g57260	*PR2*	*PATHOGENESIS-RELATED PROTEIN2*	179.9	3193.3	15.9	634.4	4.3*	5.2*	0.8218
12	At3g22600	*LTPG5*	*GPI-ANCHORED LIPID TRANSFER PROTEIN5*	15.6	775.0	1.2	81.1	5.8*	5.2*	0.8393
13	At3g26830	*PAD3*	*PHYTOALEXIN DEFICIENT3*	12.1	421.8	0.9	67.5	5.3*	5.2*	0.8512
14	At2g38240	*DOXC46*	2-Oxoglutarate-dependent dioxygenase superfamily	0.2	20.0	0.2	41.4	4.8*	5.1*	0.7480
15	At2g29350	*SAG13*	*SENESCENCE-ASSOCIATED GENE13*	27.4	1135.6	4.0	165.1	5.8*	5.0*	0.5042
16	At1g57630	–	Toll-Interleukin-Resistance domain family protein	6.2	255.9	0.9	55.9	5.3*	4.9*	0.9346
17	At2g04450	*NUDT6*	Nudix hydrolase homolog 6	35.7	623.0	2.7	102.0	4.1*	4.8*	0.9346
120	At1g75040	*PR5*	*PATHOGENESIS-RELATED PROTEIN5*	274.8	5349.1	65.7	539.2	4.3*	3.0*	0.1159
350	At4g28390	*AAC3*	*ADP/ATP CARRIER3*	15.7	165.0	5.9	25.6	3.3*	2.0*	0.0473#
510	At2g17720	*P4H5*	*PROLYL 4-HYDROXYLASE5*	28.2	188.0	18.5	58.3	2.7*	1.6*	0.0882
655	At2g19190	*FRK1*	*FLG22-INDUCED RECEPTOR-LIKE KINASE1*	2.9	70.2	0.2	1.7	4.2*	1.2*	0.3649

SAR$^+$ genes with significant *Psm*-induced upregulation in distal leaves of both Col-0 and *sid2*. The subgroup of SAR$^+$ genes (741 genes in total) is listed in descending order according to their *sid2 P*/M ratios. Asterisks indicate significant changes (FDR < 0.01). The 15 genes with the highest *P*/M-fold change in *sid2* and Col-0 $\log_2$ *P*/M values > 4.0 are depicted. Four selected genes from lower parts of the gene list are also shown. The position of each gene in the full SAR$^+$ gene list is indicated in the first column. Note that the Pip pathway genes *ALD1* and *FMO1* occur at the top of the list. P values for differences in $\log_2$ fold changes in Col-0 and *sid2* are given. Number values indicate significant differences (P < 0.05).

was observed for *GRXS13* expression, and priming for both *ARD3* and *PR1* expression was completely abolished in *sid2* (Figure 6A; Supplemental Figure 10A). Therefore, SAR induction primes *sid2* plants for enhanced expression of three members of the partially SA-independent cluster of SAR$^+$ genes, whereas priming is weak or fully absent with respect to expression of the three SA-dependent SAR$^+$ genes. In addition to gene expression, we measured priming at the metabolite level. As previously shown (Návarová et al., 2012), we found that an activated SAR state primes Col-0 plants for enhanced camalexin and SA biosynthesis upon pathogen inoculation in a Pip-dependent manner (Figure 7A; Supplemental Figure 11A). Priming of camalexin accumulation was also absent in *sid2*, indicating that both Pip and SA are required for conditioning of camalexin biosynthesis during biological SAR (Figure 7A; Supplemental Figure 11A).

Together, these results indicate that Pip is able to prime plants for enhanced activation of a subset of defense responses such as *ALD1* and *FMO1* expression during biologically induced SAR independently of SA. However, for the priming of a second category of defense responses that involve *ARD3* expression, *PR1* expression, and camalexin accumulation, both Pip and SA are necessary. Notably, our data suggest overlapping regulatory principles of SAR activation and the realization of defense priming in challenge-infected plants: Priming of expression of partially SA-independent SAR$^+$ genes can be achieved independently of SA, whereas priming of SA-dependent SAR$^+$ genes requires SA (Tables 1 and 2, Figure 6A; Supplemental Figure 10A).

Arabidopsis plants exogenously supplied with 10 µmol Pip over the root system accumulate Pip in leaves to similar levels as 2° leaves of plants exhibiting *P. syringae*-induced SAR (Návarová et al., 2012). Pip applied in this way is sufficient to enhance resistance to *P. syringae* and induces defense priming to a similar extent as biological SAR (Návarová et al., 2012). To examine the role of SA in Pip-induced defense priming, we fed Col-0, *sid2*, *ald1*, and *sid2 ald1* plants with 10 mL of 1 mM (=10 µmol) Pip, challenged leaves with *Psm* 1 d later and compared their defense responses 10 h after the challenge infection with those of unfed plants (supplied with 10 mL water). Similar to the SAR priming assay, we

Table 3. Genes Induced in Systemic Tissue of *sid2* but Not in Col-0

				Mean Expression Value				Fold Change (Log_2)	
Pos.	AGI Code	Name	Gene Name/Description	Col-0 M	Col-0 *P*	*sid2* M	*sid2 P*	*Col-0 P/M*	*sid2 P/M*
1	At5g24770	*VSP2*	*VEGETATIVE STORAGE PROTEIN2*	2.9	7.6	10.4	1108.4	1.1	6.6*
2	At5g24780	*VSP1*	*VEGETATIVE STORAGE PROTEIN1*	0.8	1.9	1.8	260.4	0.7	6.5*
3	At4g16590	*CSLA01*	*CELLULOSE SYNTHASE-LIKE A01*	0.8	1.2	1.6	133.2	0.3	5.7*
4	At1g76790	*IGMT5*	*INDOLE GLUCOSINOLATE O-METHYLTRANSFERASE5*	0.6	0.4	1.8	116.5	−0.2	5.4*
5	At4g17470	–	α/β-Hydrolase superfamily protein	1.1	2.6	2.7	148.8	0.8	5.3*
6	At2g24210	*TPS10*	*TERPENE SYNTHASE10*	0.1	0.5	0.5	54.8	0.4	5.3
7	At3g11480	*BSMT1*	*BENZOIC ACID/SALICYLIC ACID METHYLTRANSFERASE1*	0.1	0.6	0.1	40.9	0.6	5.2*
8	At1g51780	*ILL5*	*IAA-LEUCINE RESISTANT (ILR)-LIKE5*	0.0	0.4	0.1	27.8	0.5	4.8*
9	At4g13410	*CSLA15*	*CELLULOSE SYNTHASE LIKE A15*	3.8	1.0	2.6	95.5	−1.3	4.7*
10	At1g24070	*CSLA10*	*CELLULOSE SYNTHASE-LIKE A10*	1.3	1.0	1.4	55.0	−0.2	4.5*
11	At3g28220	–	TRAF-like family protein	26.3	6.5	31.2	686.5	−1.9*	4.4*
32	At3g28290	–	Sequence similarity to integrins	2.4	0.5	1.9	28.9	−1.2*	3.4*
33	At3g28300	–	Sequence similarity to integrins	1.9	0.5	2.0	29.3	−0.9*	3.3*
41	At1g52000	–	Mannose binding lectin superfamily	28.5	6.6	33.4	306.8	−2.0*	3.2*
70	At2g43550	–	Scorpion toxin-like knottin superfamily	11.8	2.1	30.5	146.1	−2.0*	2.2*
91	At5g02940	–	Protein of unknown function	109.2	32.0	148.3	464.3	−1.7*	1.6*

A total of 104 genes were identified with significant *Psm*-induced upregulation in distal leaves of *sid2* but not Col-0 plants (Figure 3A). The genes were listed in descending order according to their *sid2 P*/M ratios. The 10 genes with highest *P*/M ratios in *sid2* and all genes significantly downregulated in Col-0 (SAR^- genes) from this group are depicted. The position of each gene in the list is indicated. Asterisks indicate significant changes between *Psm* and mock treatments (FDR < 0.01).

distinguished four treatments (soil/leaf): a control situation (water/mock), Pip treatment alone (Pip/mock), pathogen challenge alone (water/*Psm*), and Pip treatment with subsequent pathogen challenge (Pip/*Psm*). We defined defense priming by analogous criteria as for the SAR priming assay (Pip/*Psm* – Pip/mock > water/*Psm* – water/mock; Supplemental Figure 9). Exogenously supplied Pip markedly intensified the *Psm*-triggered expression of *FMO1* and *ALD1* in Col-0, and this priming response was even more pronounced in *sid2* (Figure 8A; Supplemental Figure 12A). Pip feeding also primed Col-0 plants for enhanced *PR1* expression during a *Psm* challenge infection, and here, the priming effect was almost fully suppressed in *sid2* (Figure 8A; Supplemental Figure 12A). Pip-induced priming for camalexin production was also stronger in Col-0 than in *sid2* (Figure 8B; Supplemental Figure 12B). These results overlap with those of the SAR priming assay and substantiate our conclusion that Pip regulates priming for certain responses in an SA-independent manner, whereas it requires SA to mediate priming of other responses. The responses triggered by exogenous Pip were generally somewhat lower in *ald1* or *sid2 ald1* than in Col-0 plants, indicating that endogenous Pip also amplifies the priming effects in these assays (Figures 8A and 8B; Supplemental Figures 12A and 12B).

Pipecolic Acid Mediates SAR-Associated Defense Priming via *FMO1*

FMO1 is an essential component of biologically induced SAR (Mishina and Zeier, 2006). The finding that *fmo1* mutant plants are unable to increase resistance upon Pip treatment indicates that FMO1 acts downstream of Pip in SAR signal transduction (Návarová et al., 2012). To investigate the role of *FMO1* in defense conditioning, we subjected *fmo1* plants to the priming assays described above. Like *ald1*, *fmo1* plants were unable to intensify expression of partially SA-dependent or SA-independent SAR^+ genes (Figure 6B; Supplemental Figure 10B), and to potentiate camalexin and SA production in challenge-infected 2° leaves upon a previous 1° pathogen inoculation (Figure 7B; Supplemental Figure 11B). In contrast to *ald1*, however, *fmo1* was not capable of activating defense priming upon Pip feeding, because challenge-infected leaves of Pip-supplied plants were not or only very faintly able to intensify *ALD1* expression, *PR1* expression (Figure 8C; Supplemental Figure 12C), camalexin accumulation (Figure 8D; Supplemental Figure 12D), and SA biosynthesis (Supplemental Figure 13). This indicates that FMO1 is a critical mediator of Pip-activated conditioning events that determine SAR-associated defense priming.

Pip and SA Act Synergistically and Independently from Each Other to Induce *PR* Gene Expression and Disease Resistance

Exogenous SA is sufficient to induce expression of a set of defense-related genes and to confer enhanced plant resistance to different hemibiotrophic and biotrophic pathogens (Delaney et al., 1995; Sticher et al., 1997; Thibaud-Nissen et al., 2006). To examine a possible interplay of Pip and SA in the regulation of plant immune responses, we watered plants with 10 μmol Pip via the root system, subsequently infiltrated 0.5 mM SA into leaves, and determined the transcript levels of the classical SA-inducible gene *PR1* 4 h after SA treatment. Single Pip and SA applications as well as a control treatment were included, so that, as for the priming assays described above, four cases could be distinguished and

Table 4. Genes Systemically Induced in *sid2* Are Strongly Enriched in JA-Responsive Genes

Gene Category	No. of Genes	JA-Inducible Genes (%)[a]	P Value[b]
Whole gene set[c]	15,239	3.2	–
Col-0 up (SAR$^+$)	3,413	3.7	0.068
sid2 up (total)	845	12.8	$9*10^{-38}$
sid2 up/Col-0 not up[d]	104	48.1	$4*10^{-44}$

Percentage of JA-responsive genes in the total number of RNA-seq-analyzed genes and in different gene categories (as illustrated in the left Venn diagram of Figure 3A).
[a]Percentage of genes determined to be JA inducible by Goda et al. (2008).
[b]By Fisher's exact test; indicates significance of enrichment.
[c]After threshold cutoff.
[d]Genes upregulated in *sid2* but not in Col-0.

priming assessed in an analogous manner (Pip/SA – Pip/mock > water/SA – water/mock; Supplemental Figure 9). SA alone induced strong expression of *PR1* in Col-0, *ald1*, *sid2*, and *sid2 ald1* plants, indicating that elevated SA levels are sufficient to trigger *PR1* expression in the absence of Pip. However, this response was markedly fortified in all four genotypes when plants had been pretreated with Pip, indicating synergism between SA and Pip in the induction of *PR1* (Figure 9A; Supplemental Figure 14A). Furthermore, the response to SA alone was higher in the Col-0 wild type than in the other lines, suggesting that the capacity of endogenously synthesizing Pip or SA positively affects the induction of *PR1* by exogenous SA. Pip treatment alone caused increased expression of *PR1* as well. This induction was almost absent in *sid2* and in *sid2 ald1*, indicating that Pip-induced *PR1* expression depends on an intact SA biosynthetic pathway (Figure 9A; Supplemental Figure 14A).

In addition to functional *FMO1*, intact *PAD4* and *NPR1* genes are required for a strong resistance induction by exogenous Pip (Návarová et al., 2012). To get deeper mechanistic information about the synergistic interplay of Pip and SA in *PR1* induction, we examined the behavior of *fmo1*, *pad4*, and *npr1* mutant plants in our assay. SA alone triggered a strong, wild-type-like expression of *PR1* in *fmo1*. However, in contrast to the wild type, we observed neither significantly increased *PR1* expression upon Pip treatment alone nor the Pip-triggered intensification of SA-induced *PR1* expression in *fmo1* (Figure 9B; Supplemental Figure 14B). This indicates that *FMO1* acts downstream of Pip but upstream of SA in inducible *PR1* expression. Moreover, *FMO1* is required for the intensification of SA-induced *PR1* expression by Pip. Similar to *FMO1*, *PAD4* is not essential for SA-induced *PR1* expression but is required for Pip-induced *PR1* expression, indicating that *PAD4* is also positioned between Pip and SA in the signaling pathway leading to *PR1* induction. In contrast to *fmo1*, however, *pad4* was not impaired in the Pip-mediated intensification of *PR1* expression, suggesting that *PAD4* is not involved in the synergistic interplay between SA and Pip (Figure 9B; Supplemental Figure 14B). Finally, the *npr1* mutant did not show discernible expression of *PR1* after any of the treatments, indicating that *NPR1* functions downstream of both Pip and SA in the induction of *PR1* (Figure 9B; Supplemental Figure 14B).

Exogenous Pip treatment results in a significant resistance induction in Col-0, *ald1*, and *sid2* but not in *fmo1* plants (Návarová et al., 2012). Complementarily, we now tested the abilities of Col-0, *ald1*, *fmo1*, and *sid2* to augment basal resistance to *Psm* in response to exogenous SA (Figure 9C). SA treatment strongly increased resistance to *Psm* in all the genotypes. In fact, the degree of resistance induction was even higher in *ald1* and *fmo1* than in Col-0, since bacterial growth was attenuated by exogenous SA to 93 to 95% in the mutants but only to 88% in the wild type (Figure 9C). This indicates that exogenous SA can induce both *PR* gene expression (Figure 9A; Supplemental Figure 14A) and disease resistance (Figure 9C) past Pip/FMO1 signaling and points to a redundant mode of action of Pip and SA. Nevertheless, the above-described amplification of SA signaling by Pip/FMO1 (Figure 9A; Supplemental Figure 14A) was still apparent in this resistance assay, because exogenous SA restricted bacterial growth to lower absolute numbers in Col-0 than in *ald1* or *fmo1* (Figure 9C). Yet more strikingly, both Pip and SA pretreatments failed to reduce bacterial multiplication in *sid2* to the same absolute values as in the wild type (Figure 9C; Návarová et al., 2012), indicating the necessity for endogenous SA production for full resistance induction. Together, the response patterns observed here for exogenous SA and by Návarová et al. (2012) for exogenous Pip treatments place FMO1 downstream of Pip but upstream of SA in resistance induction. Exogenous SA can trigger a strong but not a complete immune response without functional Pip signaling. Reciprocally, Pip can induce a marked but not a full resistance response independently from SA biosynthesis. Together, our findings show that Pip and SA exhibit synergistic, independent, and redundant modes of action in plant immunity.

Table 5. The Transcriptional SAR Response Is Virtually Absent in *ald1*

			Mean Expression Value				Fold Change (Log_2)	
AGI Code	Name	Gene Name/Description	Col-0 M	Col-0 *P*	*ald1* M	*ald1 P*	Col-0 *P*/M	*ald1 P*/M
At4g23140	*CRK6*	*CYSTEINE-RICH RECEPTOR-LIKE KINASE6*	52.4	636.3	5.3	26.1	3.6*	2.1*
At1g14880	*PCR1*	*PLANT CADMIUM RESISTANCE1*	270.6	5673.3	7.2	29.0	4.4*	1.9*

SAR genes with significant *Psm*-induced transcript changes in distal leaves of *ald1* (FDR < 0.01). From the whole gene set, only two genes were significantly upregulated in *ald1*. Moreover, the *Psm*-induced expression values of these genes in *ald1* did not exceed the basal expression values in Col-0.

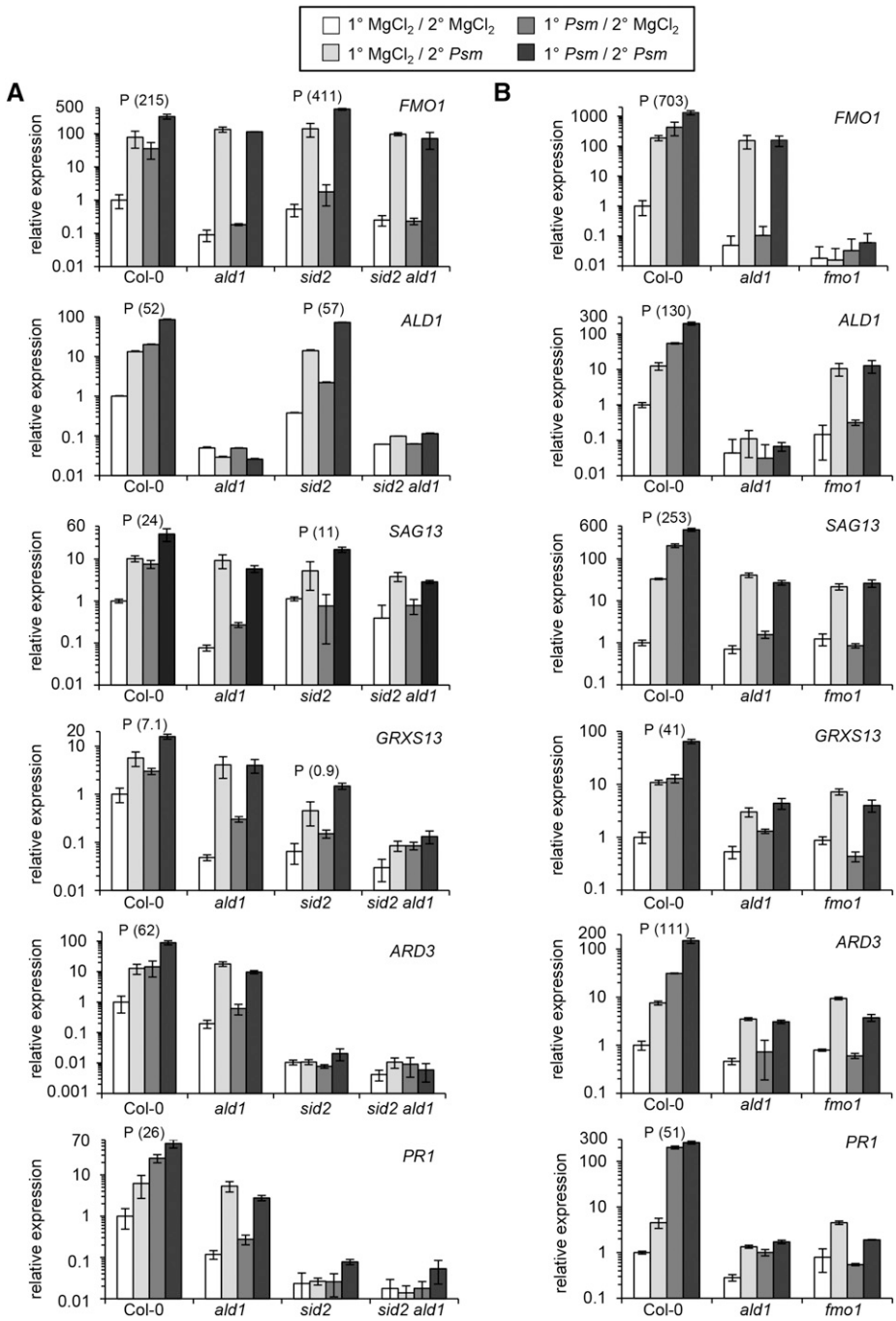

Figure 6. SAR-Associated Priming of Defense-Related Gene Expression Fully Depends on a Functional Pip/FMO1 Module but Is Only Partially SA Dependent.

(A) SAR priming assays for Col-0, *ald1*, *sid2*, and *sid2 ald1* plants.

(B) SAR priming assays for Col-0, *ald1*, and *fmo1* plants (independent experiment).

The priming assay consisted of an inductive *Psm* inoculation or mock ($MgCl_2$) treatment of 1° leaves, followed by a *Psm* challenge or mock treatment of 2° leaves 48 h later. Gene expression in 2° leaves was assessed 10 h after the second treatment (Supplemental Figure 9A). A particular defense response was defined as primed if the differences between the (1°-*Psm*/2°-*Psm*) and the (1°-*Psm*/2°-$MgCl_2$) values were significantly larger than the differences between the (1°-$MgCl_2$/2°-*Psm*) and the (1°-$MgCl_2$/2°-$MgCl_2$) values (two-sided Mann-Whitney U test, $\alpha = 0.005$) (Supplemental Figure 9B). A P above the bars for a particular genotype indicates priming. Expression of three partially SA-independent SAR$^+$ genes (*FMO1*, *ALD1*, and *SAG13*; Table 1) and three SA-dependent SAR$^+$ genes (*GRXS13*, *ARD3*, and *PR1*) were monitored. Transcript levels were assessed by quantitative real-time PCR analysis and are given as means ± SD of three biological replicates. Each biological replicate involves two technical replicates. The transcript levels are expressed relative to the respective Col-0 mock control value. Note that the graphs use a base 10 logarithmic scale for the *y* axes to ensure recognizability of both high and low values.

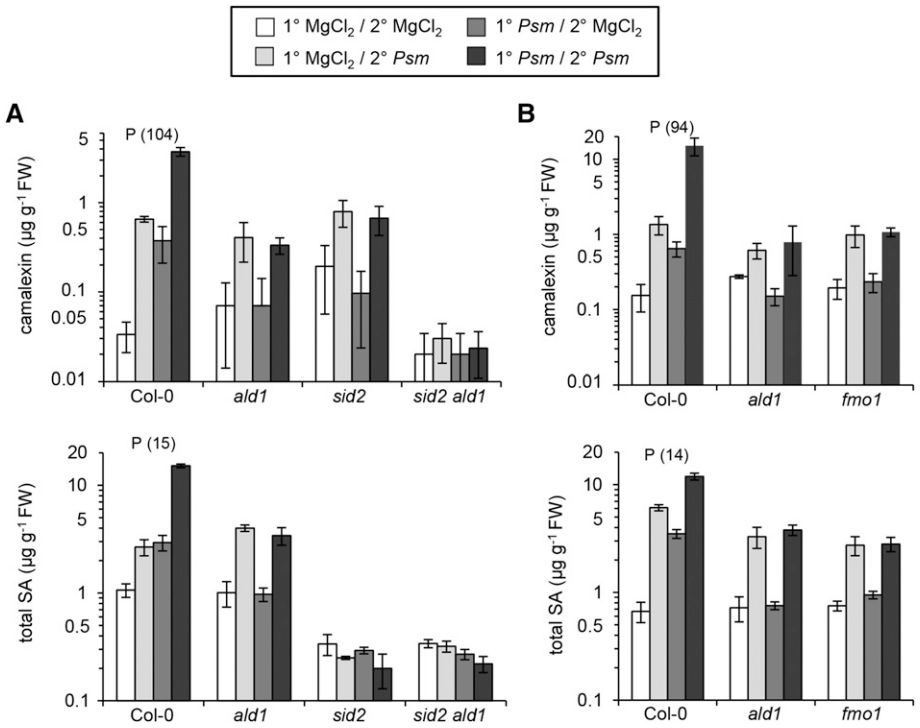

Figure 7. SAR-Associated Priming of Camalexin and SA Biosyntheses Requires a Functional Pip/FMO1 Module, and SAR Priming of Camalexin Production Is SA Dependent.

(A) SAR priming assays for Col-0, *ald1*, *sid2*, and *sid2 ald1* plants. Camalexin levels and total SA levels were determined as defense outputs. Values represent the mean ± SD of three biological replicates from different plants. Each biological replicate consists of six leaves from two plants. A P above the bars for a particular genotype indicates priming in this genotype. The prgain values are given in parentheses. Details of the priming assessments are described in the legends of Figure 6 and Supplemental Figure 9.

(B) SAR priming assays for camalexin and total SA production in Col-0, *ald1*, and *fmo1* plants, as described in **(A)**.

Note that the graphs use a logarithmic scale for the *y* axes. The same graphs with linear scaling are depicted in Supplemental Figure 11. The data sets depicted in **(A)** and **(B)** originate from independent experiments.

DISCUSSION

This study provides insights into the interplay of two key SAR regulatory plant metabolites: the phenolic SA and the non-protein amino acid Pip (Nawrath and Métraux, 1999; Wildermuth et al., 2001; Návarová et al., 2012), in SAR establishment, SAR-associated defense priming, and basal plant immunity. Key Pip and SA biosynthetic and signaling genes exhibit strong transcriptional activation upon SAR induction throughout the plant (Figure 1A; Song et al., 2004b; Mishina and Zeier, 2006; Attaran et al., 2009; Návarová et al., 2012), and both metabolites accumulate systemically in the foliage of Arabidopsis plants locally leaf-inoculated with *P. syringae*, whereby the initial rise of Pip in the systemic tissue timely precedes the increase of SA (Návarová et al., 2012). Similar to many other studies (Nawrath and Métraux, 1999; Wildermuth et al., 2001; Vlot et al., 2009), we assessed here resistance responses of the SA induction-deficient *sid2* mutant, which is defective in the pathogen-inducible SA biosynthesis gene *ICS1*, to investigate the function of SA in basal immunity and SAR. By analogy, we used *ald1* plants defective in Pip accumulation to deduce the immune responses that are regulated by Pip. Taken together, isotope labeling, biochemical, and metabolite studies strongly suggest that Pip is derived from Lys by a two-step mechanism and that ALD1 catalyzes a first aminotransferase step therein (Gupta and Spenser, 1969; Song et al., 2004a; Návarová et al., 2012; Zeier, 2013). The direct involvement of ALD1 in Pip biosynthesis and the fact that exogenous Pip can complement

Figure 6. (continued).

Graphs with a linear scale for the *y* axes, which more clearly illustrate differences between challenge-infected 1° mock-treated and 1° *Psm*-induced plants, are depicted in Supplemental Figure 10. As a measure of the gain of a response due to priming, we calculated the prgain (response gain due to priming) for each genotype with activated priming according to the formula given in Supplemental Figure 9C. prgain values are given in parentheses behind the priming indicator P and allow estimates about quantitative differences of the strength of priming between genotypes. The higher the prgain value, the stronger the priming. The data sets depicted in **(A)** and **(B)** are derived from independent experiments.

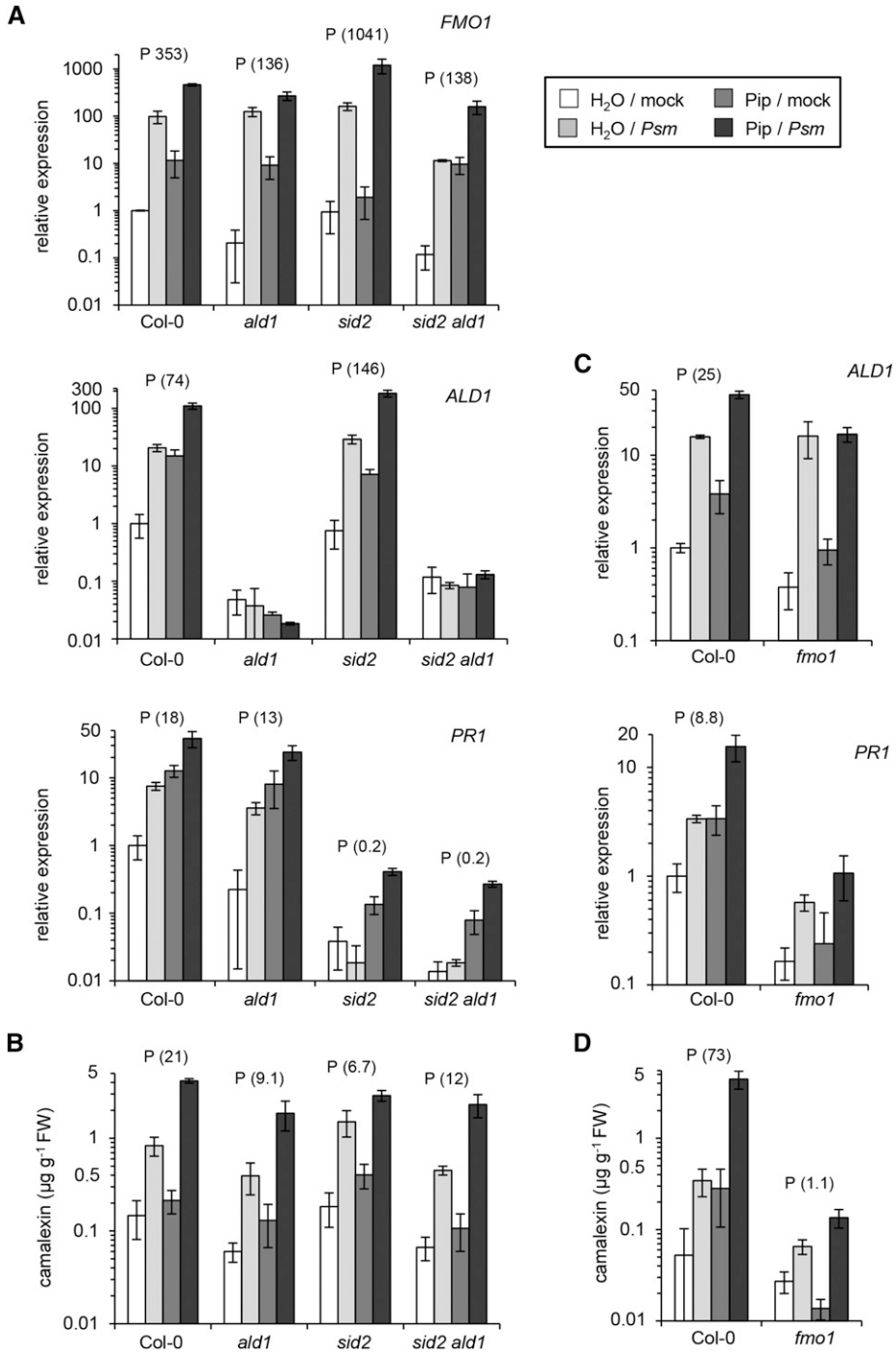

Figure 8. Exogenous Pip Confers Defense Priming in a FMO1-Dependent and Partially SA-Independent Manner.

(A) Pip-induced priming of gene expression (*FMO1*, *ALD1*, and *PR1*) in Col-0, *ald1*, *sid2*, and *sid2 ald1* plants, as determined by qPCR analysis. Plants were supplied with 10 mL of 1 mM Pip (≡ dose of 10 µmol) or with 10 mL of water (control treatment) via the root system and leaves challenge-inoculated with *Psm* or mock-infiltrated 1 d later. Defense responses in leaves were determined 10 h after the challenge treatment. Values represent the mean ± SD of three biological replicates from different plants. Each biological replicate consists of two leaves from one plant and involves two technical replicates. A P above the bars for a particular genotype indicates defense priming in this genotype, as assessed in analogy to SAR priming. The prgain values are given in parentheses (see legend to Figure 6 and Supplemental Figure 9).

(B) Pip-induced priming for camalexin production in Col-0, *ald1*, *sid2*, and *sid2 ald1* plants. Values represent the mean ± SD of three biological replicates from different plants. Each biological replicate consists of six leaves from two plants.

ald1 resistance defects (Návarová et al., 2012) suggest that, just as *sid2* is useful for SA-related research, *ald1* is a suitable genetic tool to assess the function of Pip in plants. Given the above-mentioned lines of evidence, the possibilities that metabolites other than SA and Pip (or direct derivatives thereof) substantially contribute to the *sid2* and *ald1* phenotypes, respectively, are unlikely in our opinion. Whereas the recent identification of the bona fide SA receptors NPR1, NPR3, and NPR4 (Fu et al., 2012; Wu et al., 2012) has validated that free SA is an active signal, it is not clear yet whether unmodified Pip or a direct, possibly FMO1-generated Pip derivative is signaling active (see further discussion below regarding FMO1; Zeier, 2013). In addition to the respective single mutants, we generated a Pip- and SA-deficient *sid2 ald1* double mutant as one of the tools to study the interplay between Pip and SA in basal and systemic immunity (Supplemental Figures 1 and 2).

We showed that SAR establishment in Arabidopsis is characterized by a strong transcriptional reprogramming of the systemic leaf tissue that involves robust activation of more than 3400 SAR$^+$ genes and suppression of nearly 2900 SAR$^-$ genes. Along with systemic resistance induction (Figure 2B; Song et al., 2004b; Návarová et al., 2012), this massive transcriptional SAR response is virtually absent in *ald1*, indicating that transcriptional reprogramming during SAR depends on the ability of plants to biosynthesize Pip after pathogen inoculation (Figures 1B, 3A, and 3B; Supplemental Figures 5 and 7; Návarová et al., 2012). Since knockout of *ALD1* alone is sufficient to fully abrogate the transcriptional reprogramming in distal leaves, we consider it unlikely that analogous RNA-seq analyses with the *sid2 ald1* double mutant, which we have not performed in this study, would provide mechanistic information about the transcriptional SAR response beyond that acquired for *ald1*, although we cannot fully rule out this possibility. However, in addition to *ALD1*, SAR and the transcriptional response associated with SAR fully require intact *FMO1* (Mishina and Zeier, 2006; Gruner et al., 2013). Furthermore, elevation of Pip levels by exogenous application induces a SAR-like resistance response in a FMO1-dependent manner (Návarová et al., 2012). These findings indicate that the establishment of biological SAR and the associated transcriptional reprogramming of systemic leaf tissue are regulated by a master module that involves accumulating Pip and its downstream-acting component FMO1 (Figure 10A).

Whereas the critical function of Pip for SAR has been recognized only recently (Návarová et al., 2012), it has been known for more than two decades that SA functions as another key SAR player (Vernooij et al., 1994; Nawrath and Métraux, 1999). This study confirms this assessment and shows that the extent of SAR and of the transcriptional response in systemic tissue is strongly attenuated in *sid2* plants (Figures 2B, 2C, 3A, and 3B). Our findings indicate that the degree of upregulation of the vast majority of the SAR$^+$ genes in systemic tissue is positively influenced by SA (Tables 1 and 2). However, our study adds an important aspect to the current viewpoint of SAR regulation. We show that in the absence of induced SA production, a moderate SAR and a partial transcriptional response in systemic tissue occurs upon primary bacterial inoculation (Figures 2B, 2C, 3A, and 3B). This response not only becomes apparent in the *ICS1*-defective *sid2* plants, but also in another SA induction-deficient mutant, *sid1*, which bears a defect in the multidrug and toxin extrusion-like transporter ENHANCED DISEASE SUSCEPTIBILITY5 (EDS5) (Figure 2C). EDS5 is required for the export of chloroplast-synthesized SA from this organelle, and SA accumulation in *sid1*/*eds5* is supposedly inhibited by autoinhibitory feedback (Serrano et al., 2013). Furthermore, the partial SAR response is established in *ics1 ics2*, in which both isochorismate synthase isoforms of Col-0 are inactive (Supplemental Figure 3). The *ics1 ics2* double mutant not only is impaired in stress-inducible SA biosynthesis but also displays strongly reduced basal SA levels (Garcion et al., 2008). Therefore, our study reveals the existence of an SA-independent signaling pathway that is able to activate a comparatively small but significant SAR immune response in Arabidopsis. We show that this pathway is induced upon inoculation with two inherently different bacterial pathogen types, compatible (virulent) *Psm* and incompatible (avirulent) *Psm avrRpm1*, which, in contrast to *Psm*, causes a hypersensitive cell death response in Col-0 leaves (Bisgrove et al., 1994). SAR assays conducted with the *sid2 ald1* double mutant indicate that the major, SA-dependent SAR activation pathway and the minor, SA-independent activation pathway are both regulated by Pip (Figure 2B). Therefore, the Pip/FMO1 module is able to switch on a moderate but clearly discernable SAR response in the absence of inducible SA biosynthesis (Figure 10B).

From our expression analyses we deduce that, after accumulating in systemic leaf tissue in a Pip/FMO1-dependent manner (Song et al., 2004b; Mishina and Zeier, 2006; Návarová et al., 2012), SA amplifies the expression of different SAR$^+$ genes to varying degrees (Tables 1 and 2). Systemic expression of the predominant portion of the SAR$^+$ genes shows a strict SA dependency, which signifies that these genes are not upregulated in a statistically significant manner in distal leaves of *sid2* (Figure 3A, Table 1). Paradigm examples for these strictly SA-dependent SAR$^+$ genes are *PR1*, a classical marker for the SA signaling pathway in plants and SAR establishment (Sticher et al., 1997), *ARD3*, an Arabidopsis gene with sequence similarity to a rice acireductone dioxygenase involved in the Yang cycle (Sauter et al., 2005), and *GRXS13*, encoding a glutaredoxin facilitating infection of Arabidopsis with the fungal necrotroph *Botrytis cinerea* (La Camera et al., 2011). However, about one-quarter of SAR$^+$ genes

Figure 8. (continued).

(C) Pip-induced priming assays in Col-0 and *fmo1* plants, monitoring *ALD1* and *PR1* expression. Sampling as outlined in **(A)**. The data sets depicted in **(A)** and **(C)** originate from independent experiments.

(D) Pip-induced priming assays in Col-0 and *fmo1* plants, monitoring camalexin accumulation. Sampling is outlined in **(B)**. The data sets depicted in **(B)** and **(D)** originate from independent experiments.

Note that the graphs use a logarithmic scale for the *y* axes. The same graphs with linear scaling are depicted in Supplemental Figure 12.

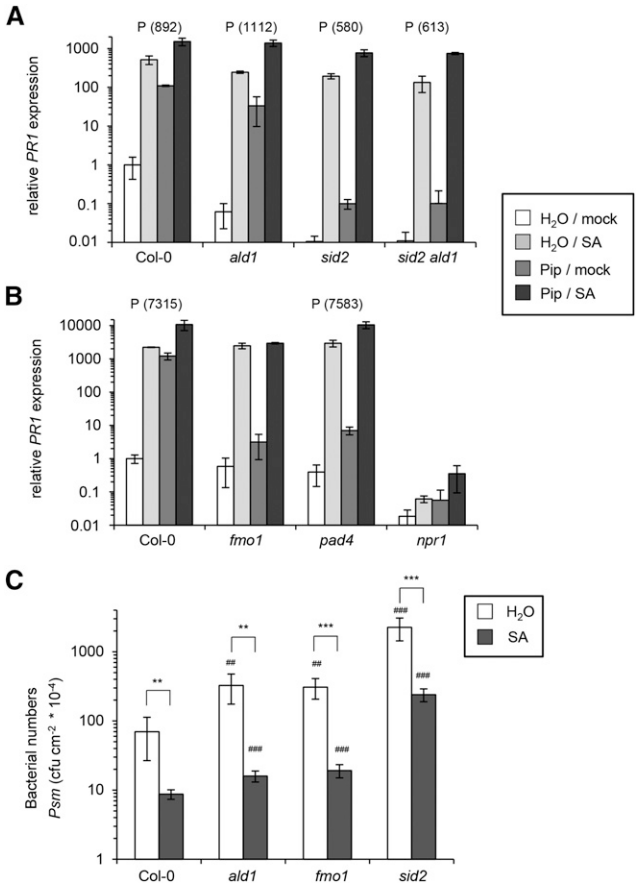

Figure 9. Pip Amplifies SA-Induced *PR1* Expression in a FMO1-Dependent Manner and Exogenous SA Enhances Basal Resistance in *ald1*, *fmo1*, and *sid2*.

(A) and **(B)** Plants were pretreated with Pip (or water) as described in the legend to Figure 8, and 1 d later 0.5 mM SA (SA) or water (mock) was infiltrated into leaves. *PR1* expression in leaves was monitored 4 h after the SA (mock) treatment by qPCR analysis. Values represent the mean ± SD of three biological replicates from different plants. Each biological replicate consists of two leaves from one plant and involves two technical replicates. *PR1* transcript levels are expressed relative to the water/mock value of Col-0. The data sets depicted in **(A)** and **(B)** originate from independent experiments. A P above the bars for a particular genotype indicates priming of SA responses in this genotype, as assessed in analogy to SAR priming. The prgain values are given in parentheses (see legend to Figure 6 and Supplemental Figure 9). Note that the graphs use a logarithmic scale for the *y* axes. The same graphs with linear scaling are depicted in Supplemental Figure 14.

(A) Col-0, *ald1*, *sid2*, and *sid2ald1*.

(B) Col-0, *fmo1*, *pad4*, and *npr1*.

(C) Basal resistance to *Psm* infection of Col-0, *ald1*, *fmo1*, and *sid2* plants is enhanced by exogenous SA. Three leaves per plant were preinfiltrated with 0.5 mM SA or water, and 4 h later, the same leaves were challenged with *Psm* (OD_{600} = 0.001). Bacterial growth was assayed 3 d later as outlined in the legend to Figure 2A. Asterisks denote statistically significant differences between SA- and water-pretreated plants (**P < 0.01 and ***P < 0.001; two-tailed *t* test). Number signs above bars of mutant values denote statistically significant differences from the respective Col-0 wild-type value (##P < 0.01 and ###P < 0.001; two-tailed *t* test).

were significantly upregulated in the systemic leaf tissue of *sid2* upon 1° inoculation and showed higher absolute expression values in *Psm*-inoculated *sid2* mutants than mock-treated Col-0 plants (Figure 3A, Table 2). These genes require SA for their full expression in systemic tissue but can be induced to different degrees without SA elevation. Notably, the two SAR regulatory and Pip pathway genes *ALD1* and *FMO1* rank among the SAR^+ genes with the strongest SA-independent expression characteristics (Table 2). This suggests that the Pip signaling pathway can function separately from SA to switch on a subset of systemic resistance responses to a certain level. Nevertheless, for a full and strong SAR response, accumulation of SA is required to potentiate these partially SA-independent responses that include Pip production and signaling and to turn on other, strictly SA-dependent responses such as *PR1* expression (Figures 10A and 10B).

Functional *ICS1* is not a sufficient prerequisite for pathogen-induced SAR, as exemplified by the full SAR defects of *ald1* and *fmo1* (Figure 2B; Song et al., 2004b; Mishina and Zeier, 2006; Návarová et al., 2012). This is the case because Pip biosynthesis and signal transduction via *FMO1* are required to switch on virtually every response in distal leaves of locally inoculated plants, including the expression of *ICS1*, SA biosynthesis, and SA downstream responses (Figures 1B, 1C, 3B, and 10A to 10C; Mishina and Zeier, 2006; Gruner et al., 2013). However, once SA levels elevate in leaves, significant SA responses can be activated in the absence of a functional Pip/FMO1 module. This is experimentally revealed in *ald1* and *fmo1* plants exogenously supplied with SA because these plants exhibit markedly enhanced expression of *PR-1* and elevated resistance to *Psm* (Figure 9). This aspect is relevant for defense processes in inoculated leaves because here, in contrast to distal leaves, pathogen-induced *ICS1* expression and SA accumulation are still active in *ald1* and *fmo1* (Figures 1A and 1C; Song et al., 2004b; Mishina and Zeier, 2006; Bartsch et al., 2006). Our findings that SA-deficient *sid2* plants exhibit a more pronounced defect in local resistance to *Psm* than *ald1* or *fmo1* (Figures 2A and 9C) indicate that the contribution of the SA pathway to basal immunity exceeds that of the Pip/FMO1 pathway. A largely Pip/FMO1-independent activation of the SA defense pathway at pathogen inoculation sites might explain why defects in Pip biosynthesis and *FMO1* result in comparatively moderate decreases of basal immunity. In fact, the importance of *FMO1* for local plant immune responses is variable and depends on the nature of the attacking pathogen, with particular significance of *FMO1* for local immunity to pathogens that activate *EDS1*-dependent and SA-independent branches of plant defense (Bartsch et al., 2006; Koch et al., 2006). Interestingly, EDS1 and its interacting partner PAD4, both master regulators of basal immunity (Feys et al., 2001), have also been identified as necessary SAR components (Mishina and Zeier, 2006; Jing et al., 2011; Rietz et al., 2011; Breitenbach et al., 2014). PAD4 positively regulates the transcription of a whole battery of defense genes including the SAR-relevant genes *ALD1*, *FMO1*, and *ICS1* (Zhou et al., 1998; Jirage et al., 1999; Song et al., 2004b; Bartsch et al., 2006). Therefore, overlapping regulatory principles of basal immunity and SAR exist. However, the relevance of the Pip/FMO1 module for SA pathway activation seems to be a main distinguishing feature of the resistance modes at sites of *Psm* attack and in distal tissue (SAR). Whereas the Pip/FMO1 module possesses an

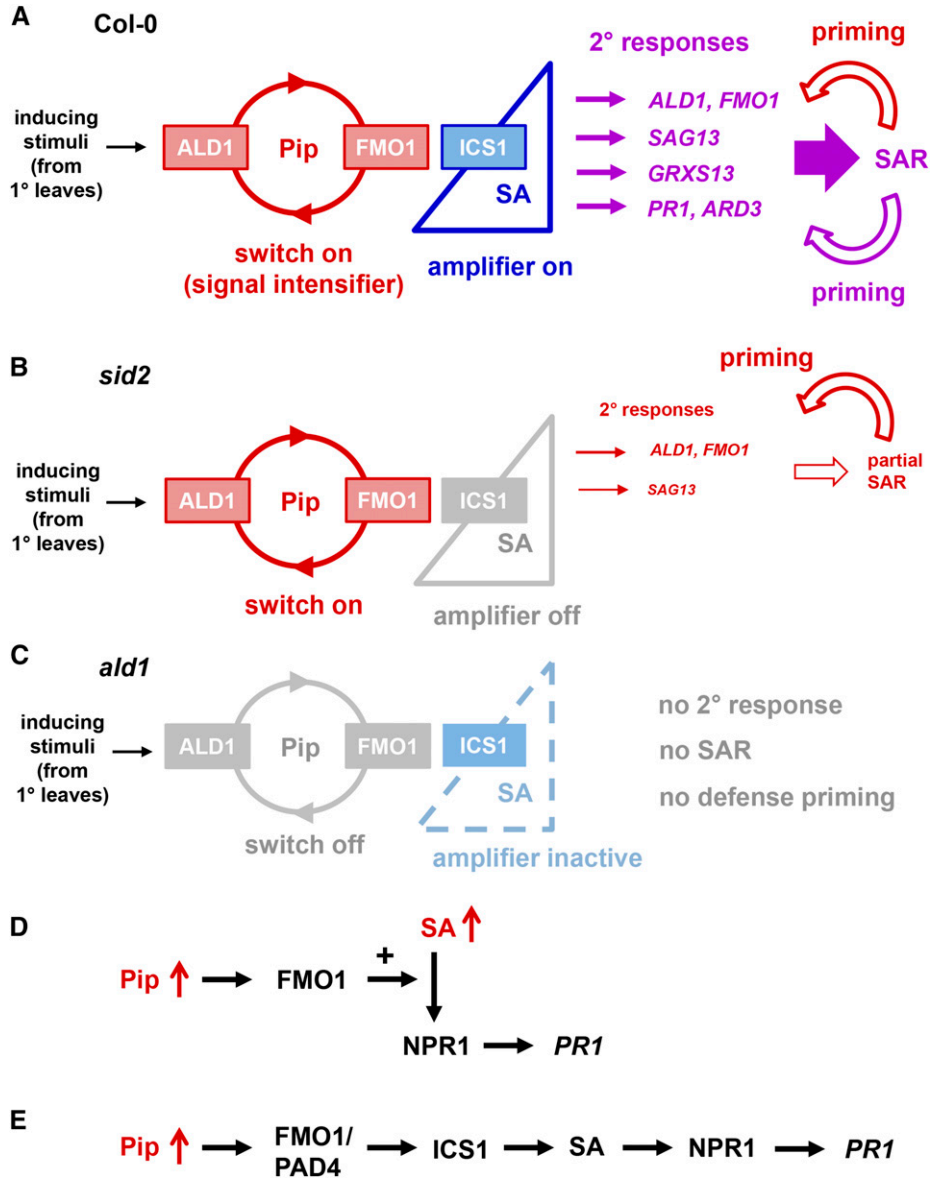

Figure 10. Summary of the Roles of Pip, FMO1, and SA in Arabidopsis SAR and Associated Defense Priming, and Modes of the Synergistic Interplay between Pip and SA.

(A) to **(C)** Regulation of the SAR transcriptional response, SAR establishment, and SAR-associated defense priming by Pip, FMO1, and SA.
(A) The situation in wild-type plants. The full SAR and priming responses are established by elevated levels of ALD1-generated Pip, the action of FMO1 downstream of Pip, and ICS1-synthesized SA in 2° leaf tissue. The Pip/FMO1 module acts as an indispensable switch for SAR activation, and SA amplifies Pip-dependent responses to different degrees.
(B) The situation in *sid2* mutant plants. In the absence of functional ICS1 and elevated SA, the Pip/FMO1 module is sufficient to induce a set of partially SA-independent responses to a certain level and trigger a moderate SAR response. Notably, an intact Pip/FMO1 module is also capable to prime plants for enhanced activation of partially SA-independent responses in the absence of SA elevations (bent red arrow).
(C) The situation in *ald1* and *fmo1* mutant plants. Functional ICS1 alone is not sufficient for SAR activation. Without Pip elevations or functional FMO1, SA biosynthesis is not activated. Failure of both Pip and SA elevations prevents the establishment of a primed state. Without the Pip/FMO1 module, inducing stimuli from 1° leaves are either not transduced into a meaningful response in 2° leaves or too weak to induce a noticeable response.
(D) and **(E)** Two modes of synergistic interplay between the immune signals Pip and SA.
(D) Elevated Pip levels amplify SA-induced *PR1* expression. This amplification response is mediated by FMO1 but does not depend on PAD4.
(E) Elevated Pip levels induce *PR1* expression via ICS1-triggered SA production. This signaling mode of Pip depends on both FMO1 and PAD4.

obligate switch function for SAR activation, it seems to play a supportive but less rigorous role for resistance induction at inoculation sites.

Notably, our resistance assays with *sid2 ald1* reveal that the SA and Pip defense pathways provide additive, independent contributions to Arabidopsis basal resistance toward *Psm* infection (Figure 2A). This is further corroborated by the findings that exogenous Pip is able to enhance resistance of *sid2* to *Psm* (Návarová et al., 2012) and that exogenous SA increases resistance of *ald1* to *Psm* (Figure 9C). Moreover, Bartsch et al. (2006) have shown that a *sid2 fmo1* double mutant is more susceptible to the *Hyaloperonospora arabidopsidis* isolate Cala2, an avirulent oomycete pathogen that is recognized by the RPP2 resistance protein in the Arabidopsis accession Col-0 than either *sid2* or *fmo1* single mutants. This indicates additive contributions of the SA and Pip/FMO1 pathways also in resistance gene-mediated responses.

However, our data also show a synergistic relationship between Pip and SA signaling on several levels. First, application of Pip intensifies *PR1* expression induced by exogenous SA in a FMO1-dependent manner (Figures 9A, 9B, and 10D; Supplemental Figures 14A and 14B). This enhancement, which also takes place in SA-deficient *sid2* (Figure 9A), indicates that the Pip/FMO1 module amplifies SA downstream signaling events. Second, elevated Pip levels trigger *PR1* expression via the induction of SA biosynthesis (Figure 10E), as indicated by both the shortcoming of *sid2* to induce *PR1* upon exogenous Pip feeding (Figure 9A) and the ability of exogenous Pip to moderately induce SA accumulation in Arabidopsis (Návarová et al., 2012). Pip therefore acts both upstream of SA to trigger *PR1* expression and downstream of SA to fortify SA-induced *PR1* expression (Figures 10D and 10E). The SA-mediated, *PR1*-inducing action of Pip as well as its function as an SA signal intensifier share overlapping mechanisms because both functions require functional *FMO1* and operate upstream of NPR1. However, both operation modes of Pip also differ mechanistically because the *PR1*-inducing but not the intensifying mode requires PAD4 (Figures 9B, 10D, and 10E). Complementary to these positive effects of Pip on SA biosynthesis and signaling, SA feeding alone is sufficient to trigger small but significant elevations of *ALD1* expression and Pip levels (Návarová et al., 2012). These findings exemplify that, in addition to their above-described independent modes of action, the Pip and SA pathways mutually reinforce each other in the regulation of plant immunity and SAR.

Crosstalk between different stress-related plant signals is well established (Derksen et al., 2013). For example, synergism between JA and ethylene signaling ensures effective induction of plant defenses directed against necrotrophic pathogen attack (Memelink, 2009). Moreover, the JA/ethylene and SA signaling pathways negatively influence each other to prioritize specific defense outputs in plant-pathogen interactions (Koornneef and Pieterse, 2008; Zander et al., 2014). JA biosynthesis and signaling is strongly induced by *P. syringae* infection in inoculated leaves. However, activation of the JA pathway is variable and strongly correlates with necrotic tissue disruption but not with systemic responses or SAR (Mishina and Zeier, 2007; Zoeller et al., 2012). With the inoculation conditions to induce SAR used in this study, JA biosynthesis and expression of JA-responsive genes are not elevated in systemic tissue of Col-0 wild-type plants (Table 4; Gruner et al., 2013). Although a considerable systemic JA response in Arabidopsis early after inoculation with high titers of avirulent *P. syringae* has been detected and associated with SAR (Truman et al., 2007), genetic analyses argue against a role of the JA pathway in Arabidopsis SAR establishment (Chaturvedi et al., 2008; Attaran et al., 2009). Notably, our comparative RNA-seq analyses reveal that distal leaves of locally inoculated *sid2* plants express JA-responsive genes to a significantly higher extent than Col-0 plants. In particular, the genes that were upregulated in *sid2* but not changed or downregulated in Col-0 are markedly enriched in JA-inducible genes (Table 4). This indicates that the accumulation of SA during SAR in wild-type plants suppresses systemic JA responses and directly illustrates the occurrence of SA/JA antagonism within SAR. The apparent prevalence of SA over JA signaling in SAR-induced plants might explain why SAR provides protection particularly against pathogens with a (hemi)biotrophic lifestyle (Sticher et al., 1997). Potential crosstalk of Pip with plant stress signals and hormones other than SA is not yet established. However, a recent study reports that treatment of Arabidopsis seedlings with methyl jasmonate decreases *ALD1* expression and Pip levels in roots, indicating negative influences of JA on Pip biosynthesis (Yan et al., 2014).

SAR can condition plants to induce defense responses more quickly and efficiently after pathogen challenge (Jung et al., 2009; Návarová et al., 2012), a phenomenon designated as defense priming (Conrath, 2011). Within our experimental setup, we defined a particular defense response as primed, if the difference between the pathogen and mock response of SAR-activated (or Pip-stimulated) plants is significantly larger than the same difference of nonactivated plants (Supplemental Figure 9B), resulting in the strongest absolute response level in pathogen-challenged, SAR-activated (or Pip-stimulated) plants (Figures 6 to 8; Supplemental Figures 10 to 12). This does not mean that the pathogen-triggered fold change of the response in SAR- (Pip-) activated plants is larger than the respective fold change in control plants. For example, in the SAR-priming assay shown in Figure 6A (Supplemental Figure 10A), the quotient between the averaged 1°-*Psm* /2°-*Psm* to the averaged 1°-*Psm* /2° mock expression value for *GRXS13* is 5.2 for the Col-0 wild type, whereas the quotient between the 1°-mock/2°-*Psm* to the 1°-mock/2°-mock value is 5.7. Therefore, an important determinant of the response gain due to priming is the marked increase of the response level caused by the inducing stimulus alone (SAR activation and Pip stimulation). A further increase of a strongly preelevated response level due to 2° challenge will ultimately lead to a much stronger absolute response level than a similar increase from a very small level present in noninduced plants. This mechanistic aspect of priming is consistent with a general model of the priming phenomenon proposed by Bruce and colleagues for two subsequent stress exposures (Bruce et al., 2007).

Between independent SAR or Pip induction experiments, the observed priming patterns in wild-type plants are reproducible and can be tested with our proposed algorithm (Supplemental Figures 9B and 9C). However, absolute or relative measurement values resulting from one of the four treatment cases (e.g., mock/mock, mock/*Psm*, *Psm*/mock, or *Psm*/*Psm*) might quantitatively vary between experiments (for example, compare Figures 6A with

6B, 7A with 7B, or Figures 8A/8B with 8C/8D). In this context, we performed linear model-based analyses of the SAR-associated priming responses (Figures 6 and 7), the Pip-induced priming responses (Figure 8), and the Pip-mediated intensification of SA-inducible *PR1* expression (Figures 9A and 9B) in the Col-0 wild type using combined data of three independent experiments to estimate treatment and experimental effect terms (Supplemental Tables 1 to 3). In doing so, we assumed that priming in our assays corresponds to the interaction of a pretreatment (treatment 1) on the response of a second treatment (treatment 2). These analyses confirm that, although experimental variation significantly influences the individual treatment responses and the interaction term (priming) for most measured values, the individual treatment responses and the priming response are stable over different experiments (Supplemental Tables 1 to 3).

Besides microbial encounters, adverse abiotic conditions can prime plants for enhanced pathogen responses (Singh et al., 2014). For more than two decades, SA has been attributed an important role in defense priming. For instance, in leaf tissue directly adjacent to pathogen attack, SA has been implicated in the potentiation of expression of defense genes that are not directly SA responsive (Mur et al., 1996). Furthermore, exogenous SA or pretreatment with chemicals such as 2,6-dichloroisonicotinic acid or *S*-methyl-1,2,3-benzothiadiazole-7-carbothioate (BTH), which are often vaguely designated as SA analogs, are able to prime cultured plant cells or intact plants for enhanced defense responses (Kauss et al., 1992; Thulke and Conrath, 1998), and BTH-induced priming proceeds via the SA downstream regulator NPR1 (Kohler et al., 2002). Moreover, treatments with chemicals that inhibit SA glycosylation and thereby endogenously elevate free SA levels lead to priming responses in Arabidopsis (Noutoshi et al., 2012), and defense priming triggered by exogenous β-amino butyric acid or the bacterial quorum sensing compound *N*-acyl-homoserine lactone requires an intact SA signaling pathway (Zimmerli et al., 2000; Schenk et al., 2014). Our study reveals a differentiated role of SA in the defense priming responses associated with SAR: SA is required to prime plants for enhanced activation of certain defense responses but is dispensable for the potentiation of others. On the one hand, genes such as *PR1*, *ARD3*, and *GRXS13*, which we had classified as SA dependent according to their expression characteristics in systemic tissue upon SAR induction, also require SA accumulation for augmented expression during challenge infection (Figure 6A). On the other hand, the expression of the partially SA-independent SAR genes *ALD1*, *FMO1*, and SAG13 is potentiated in the SAR priming assays to a similar extent in Col-0 and *sid2*, and a primary inoculation thus primes plants for enhanced expression of these genes in an SA-independent manner in systemic tissue (Figure 6A).

Our previous work identified Pip as a critical regulator of SAR-associated defense priming in Arabidopsis (Návarová et al., 2012). Exogenous Pip also increases resistance of tobacco plants to *P. syringae* pv *tabaci* and primes plants for early SA accumulation, indicating a conserved role of Pip in plant defense priming (Vogel-Adghough et al., 2013). This study shows that Pip elevations in leaves are both required and sufficient for the priming of both SA-dependent and -independent SAR responses (Figures 6 to 8; Supplemental Figures 10 to 12). Moreover, our results provide evidence that, in addition to Pip, functional FMO1 is essential for the SAR-associated priming phenomenon (Figure 6B). In fact, FMO1 acts downstream of Pip in the activation of defense priming because the priming responses induced by exogenous Pip are virtually blocked in *fmo1* (Figure 8B; Supplemental Figure 13). This finding is consistent with the critical role of FMO1 for SAR and resistance induction by Pip (Mishina and Zeier, 2006; Návarová et al., 2012; Gruner et al., 2013). Future work should focus on the biochemical function of the flavin monooxygenase FMO1. A conceivable scenario is that FMO1 catalyzes the oxidation of Pip or a Pip-derived metabolite for defense signal transduction (Zeier, 2013).

The existence of SA-independent defense priming responses associated with SAR parallel recent findings on silicon-induced resistance in Arabidopsis, in which increased silicon absorption primed plants for effective responses also in a *sid2* background (Vivancos et al., 2015). Moreover, SA-independent SAR activation, which is moderate for Arabidopsis (Figures 2B and 2C), might be more pronounced in monocots, as activation of systemic immunity in barley by leaf inoculation with bacterial pathogens has been shown to proceed in an NPR1-independent manner (Dey et al., 2014). Which molecular components besides Pip and FMO1 could be involved in the SA-independent signaling pathway leading to partial SAR and defense priming in Arabidopsis? Recent data point to a role of mitogen-activated protein kinase (MAPK) signaling cascades in the activation of SA-independent resistance responses and SAR. On one hand, Tsuda and colleagues have shown that a sustained activation of mitogen-activated protein kinase 3 (MPK3) and MPK6 in leaves of transgenic Arabidopsis plants results in the induction of *PR1* and other SA-responsive genes in *sid2* and *npr1*, indicating that strong activation of MAPK signaling can induce defense gene expression independently of a functional SA pathway (Tsuda et al., 2013). *PR1* induction in systemic leaf tissue of *P. syringae*-inoculated plants, however, is strictly SA dependent (Table 1), indicating differences between the SA-independent branch of biological SAR and the SA-independent signaling pathway activated by sustained MAPK expression (Tsuda et al., 2013). Nevertheless, Beckers et al. (2009) reported that priming of abiotic stress responses and SAR are compromised in a *mpk3* mutant and attenuated in *mpk6*, indicating a role for MAPK3/6 signaling in SAR. In our SAR analyses, several MAPK, MAPK kinase, and MAPK kinase kinase genes are significantly upregulated upon SAR induction (Figure 4F), including *MPK3* and *MPK6*. In *sid2*, however, systemic upregulation of MAPK cascade genes is only weakly induced, suggesting that transcriptional activation of these genes is largely SA dependent (Supplemental Figure 15). Future experiments should further dissect the role of MAPK signaling in SAR and, in particular, clarify its relationship to the Pip signaling pathway.

Our RNA-seq data suggest that SAR prepares plants for future pathogen attack by the transcriptional preactivation of different, consecutive stages of defense signaling. First, a widespread upregulation of genes putatively involved in pathogen recognition and early signal transduction occurs upon SAR establishment. For example, many Toll-interleukin-1 receptor-like domain (TIR)-NBS-leucine rich repeat (LRR) or coiled coil (CC)-NBS-LRR-type resistance proteins are upregulated upon SAR activation (Figure 4E; Supplemental Figure 15). These include *VICTR*, which encodes a TIR-NBS-LRR protein that associates with EDS1 and PAD4 in

protein complexes and is required for small molecule-mediated crosstalk between abscisic acid and immune signaling (Kim et al., 2012). Furthermore, genes coding for receptor-like proteins and members of specific receptor-like kinase families prominently occur in the SAR$^+$ gene group (Figure 4E). For instance, cysteine-rich protein kinase (CRK) genes are widely upregulated upon SAR establishment. Dexamethasone-inducible expression of *CRK13* in Arabidopsis, one of the most strongly upregulated CRK genes during SAR (Supplemental Figure 15), resulted in increased SA-mediated resistance to *P. syringae* (Acharya et al., 2007). These results suggest that the increased, broad-spectrum expression of resistance proteins and pattern recognition receptors during SAR is an integral part of systemic resistance activation and defense priming. Moreover, the well-characterized pattern recognition receptor genes *EFR*, *BAK1*, and *CERK1*, but not *FLS2* (Zipfel, 2014), are among the SAR$^+$ genes (Supplemental Figure 15). SA has been shown to dynamically regulate the levels of FLS2 and BAK1 and to promote their upregulation at later signaling stages (Tateda et al., 2014). Consistent with the notion that SA positively regulates microbial pattern receptors, *sid2* shows strongly reduced upregulation of these genes. However, a marked SA-independent (but Pip-dependent) component of receptor upregulation is discernable, as exemplified by increased systemic expression of several *CRK* genes in *sid2* (Supplemental Figure 15).

Besides the above-discussed MAPK members, several other gene types involved in signaling steps downstream of pathogen perception are broadly activated in systemic tissue of SAR-induced plants. These include genes coding for Ca^{2+} signaling-related proteins such as calcium-dependent protein kinases, EF-hand-containing proteins, and calmodulin binding proteins (Figure 4G). Among those is CPK5 (Supplemental Figure 15), an Arabidopsis calcium-dependent protein kinase that phosphorylates the NADPH oxidase isoform RbohD (Respiratory burst oxidase homolog D). CPK5 is required for the rapid leaf-to-leaf propagation of defense responses upon PAMP perception, and reactive oxygen species-mediated cell-to-cell communication involving CPK5 and RbohD has been suggested as a basis for long-distance defense signal propagation (Dubiella et al., 2013). However, a direct function of CPK5 in pathogen-induced SAR has not yet been established.

Many immune-related signal transduction pathways culminate in the activation of transcription factors and cofactors in the nucleus and thereby trigger enhanced expression of defense-related genes. The transcriptional coactivator NPR1 acts as a central transducer of SA responses and is essential for biological SAR as well as for SAR-related transcriptional responses (Fu and Dong, 2013). For example, NPR1 is required for the expression of ~98.5% of BTH-inducible genes (Wang et al., 2006). It is likely that NPR1 also largely regulates, besides the SA-dependent SAR activation pathway, also the Pip-dependent and partially SA-independent branch of SAR induction described here, because exogenous Pip induces a much weaker resistance response in *npr1* than in *sid2* (Návarová et al., 2012). NPR1 interacts with different members of the TGA subfamily of bZIP transcription factors to regulate *PR* gene expression (Fu and Dong, 2013). *NPR1*, its paralog *NPR3*, and three TGA genes (*TGA5*, *TGA3*, and *TGA1*) are SAR$^+$ genes showing a moderate but significant degree of upregulation upon SAR induction (Supplemental Figure 15).

Remarkably, more than one-third of the WRKY family of transcription factors belong to the SAR$^+$ group, suggesting that WRKY factors play a major role in the SAR transcriptional response (Figure 4H). For many WRKYs, positive or negative regulatory roles in distinct plant immune responses have been established (Pandey and Somssich, 2009). Among the SAR$^+$ genes are several WRKY factor genes whose BTH-induced expression depend on NPR1 (Supplemental Figure 15; Wang et al., 2006). WRKY18, for example, controls about one-fourth of BTH-induced and NPR1-regulated genes in Arabidopsis, indicating that individual WRKY factors regulate expression of subgroups of the SAR transcriptome (Wang et al., 2006). Interestingly, the marked upregulation of WRKY genes correlates with an enrichment of VQ motif-containing genes in the SAR$^+$ group (Supplemental Figure 8B). VQ motif-containing proteins have been shown to interact with WRKY proteins and appear to be part of transcriptional regulatory protein complexes in plant immunity (Cheng et al., 2012). Besides WRKYs and TGAs, NAC transcription factors are overrepresented in the SAR$^+$ gene group, whereas other classes are not (Figure 4H). This suggests a dominant function of particular transcription factor families in mediating the SAR transcriptional response. Sequential waves of specific transcription factor activities have been suggested to orchestrate plant immunity (Moore et al., 2011), and this might be particularly true for SAR activation. For the initiation of this transcriptional program leading to SAR, the Pip/FMO1 module and the transcriptional coregulator NPR1 are indispensable.

Our results not only illustrate that SAR equips plants with an increased defense capacity at different signaling levels, but also show that the state of increased pathogen resistance is associated with a diminished photosynthetic rate systemically in the foliage and strongly decreased expression of photosynthesis-related genes (Figures 4A and 5A; Supplemental Figure 5 and Supplemental Data Set 2). Moreover, the transcriptional SAR response illustrates an overall decline of several anabolic pathways, secondary metabolism, cell wall remodeling, and wax and cutin biosynthesis (Figures 4A to 4C; Supplemental Data Set 2), suggesting that SAR is associated with reduced plant growth. The induced decline in photosynthetic rates is completely absent in both *ald1* and *sid2* (Figure 5A), indicating that the Pip-dependent accumulation of SA attenuates photosynthesis systemically in the plant. This interpretation is consistent with the observation that plants exhibiting constitutively high SA levels show decreased efficiency of several photosynthetic parameters (Mateo et al., 2006). Similarly, enhanced SA levels during SAR appear to trigger growth alleviation because transcriptional gene downregulation is strongly suppressed in *sid2* (Figure 5A) and plants with high constitutive SA levels exhibit retarded growth (Bowling et al., 1997; Mauch et al., 2001). The decrease in photosynthesis (and growth) might be a consequence of reduced stomatal conductance in SAR-activated plants, as the decreases in transpiration rates indicate (Figure 5B). This would in turn limit CO_2 uptake and carbon fixation. Since the transpiration rates do not systemically decrease in *ald1* and *sid2* (Figure 5B), and exogenous SA is able to induce stomatal closure in Arabidopsis (Zeng et al., 2011), accumulating SA during SAR also likely accounts for this phenomenon. A closure of stomata represents an integral part of the PAMP-induced immune response of plants to bacterial pathogen entry (Melotto et al., 2006), and our data suggest that the stomatal

defense response is also preactivated systemically in the foliage upon localized pathogen encounter.

In conclusion, Arabidopsis SAR and the associated defense priming phenomenon are master-regulated by Pip accumulation and the action of FMO1 downstream of Pip. The Pip/FMO1 switch module activates SA-dependent and SA-independent responses that both contribute to SAR establishment and the execution of defense priming. SA amplifies Pip/FMO1-dependent responses to different degrees and thereby ensures strong SAR and priming reactions. This work further indicates that Pip and SA cooperatively interact but can also function independently from each other in the induction of plant immune responses.

METHODS

Plant Material and Cultivation

Arabidopsis thaliana plants were grown individually in pots containing a mixture of soil (Substrat BP3; Klasmann-Deilmann), vermiculite, and sand (8:1:1) in a controlled cultivation chamber with a 10-h-day (9 AM to 7 PM; PFD 100 µmol m^{-2} s^{-1})/14-h-night cycle and a relative humidity of 70%. Day and night temperatures were set to 21°C and 18°C, respectively. Experiments were performed with 5- to 6-week-old, naïve plants exhibiting a uniform appearance.

The *ald1* and *fmo1* mutants represent the SALK lines SALK_007673 and SALK_026163, respectively (Mishina and Zeier, 2006; Návarová et al., 2012). *sid2-1* (*sid2*, *ics1*; Nawrath and Métraux, 1999), *ics1 ics2* (Garcion et al., 2008), *npr1-2* (*npr1*, NASC ID: N3801), and *pad4-1* (*pad4*; Jirage et al., 1999) were used in this study. All mutant lines are in the Col-0 background.

The *sid2-1 ald1* (*sid2 ald1*) double mutant was generated by crossing of the *sid2-1* (female parent) and *ald1* (male parent) single mutants. From every fertilized silique, the F1 seeds were collected individually and dried before planting. About 110 *sid2 ald1* candidate plants were analyzed in the F2 generation as outlined in Supplemental Figures 1 and 2. One positive F2 candidate (*sid2 ald1* #6) was self-pollinated and used for experiments. The position of the ethyl methanesulfonate-generated mutation in *sid2-1* results in a stop codon (TAA) at residue 449 instead of a glutamine (Wildermuth et al., 2001). To identify the ethyl methanesulfonate-generated mutation, site specific primers were designed and the specific annealing temperature of 64°C determined in a gradient PCR. To identify the homozygous T-DNA insertion of *ald1* by PCR, the method described by Alonso et al. (2003) was applied, using gene-specific primers (Supplemental Table 4). Seeds of *ics1 ics2* were sterilized and germinated on full Murashige and Skoog medium containing 2% sucrose (pH 5.7) before the seedlings were transferred to soil (Garcion et al., 2008).

Cultivation of Bacteria

Psm and *Psm* harboring the *avrRpm1* avirulence gene (*Psm avrRpm1*) were cultivated at 28°C in King's B medium to which appropriate antibiotics were added (Zeier et al., 2004). Overnight log phase cultures were diluted to different final optical densities at 600 nm (OD_{600}) for leaf inoculations. As experimentally determined, OD_{600} = 1 corresponds to $3.2*10^8$ colony-forming units per mL.

SAR Experiments, Defense Priming, and Plant Basal Resistance

To activate SAR, plants were infiltrated between 10 and 12 AM into three lower (1°) leaves with bacterial suspensions of OD_{600} = 0.005. Infiltration with 10 mM $MgCl_2$ served as the mock control treatment. Upper (2°) leaves were harvested 48 h after the primary treatment for the determination of systemic gene expression and metabolite contents, as well as for RNA-seq analyses. For systemic resistance assays, 2° leaves were inoculated with *Psm* (OD_{600} = 0.001) 2 d after the 1° treatment. The number of *Psm* bacteria in 2° leaves was assessed another three days later as described in Návarová et al. (2012). SAR-associated defense priming was assessed by challenging 2° leaves with either *Psm* (OD_{600} = 0.005) or infiltrating 10 mM $MgCl_2$ as a mock control 2 d after the 1°-inducing or 1° mock treatments. The 2° leaves were collected 10 h later for analyses (Supplemental Figure 9). For the determination of basal resistance, suspensions of *Psm* (OD_{600} = 0.001) were infiltrated into three full-grown leaves of naive plants. Bacterial growth was assessed 3 d later (Návarová et al., 2012).

Exogenous Treatments with Pip and/or SA

Exogenous Pip was applied to plants by pipetting 10 mL of a 1 mM (10 µmol) D,L-pipecolic acid solution (S47167; Sigma-Aldrich) onto the soil substrate of individually cultivated plants. Control plants were supplemented with 10 mL of water instead. Pip feeding in this way served as the inducing treatment for Pip-priming assays. The bacterial challenge was performed 1 d after Pip application as described for the SAR priming assay. To determine synergism between Pip and SA, SA was infiltrated into leaves in a concentration of 0.5 mM 1 d after Pip feeding, and water infiltration served as a mock control. Leaf samples were collected 4 h after treatment.

Metabolite Determination

Determination of Pip levels in leaves was performed by a protocol detailed by Návarová et al. (2012), using gas chromatography-mass spectrometry-based analysis following propyl chloroformate derivatization. Free SA, conjugated SA, and camalexin were determined by a method based on vapor-phase extraction and gas chromatography-mass spectrometry analysis of metabolites as described by Attaran et al. (2009) and Návarová et al. (2012).

Quantitative Real-Time PCR Analysis

Quantitative real-time PCR (qPCR) analysis to assess gene expression in leaves was performed as detailed by Návarová et al. (2012) with minor modifications. In brief, 1 µg total RNA extracted with PeqGOLD RNAPure reagent (PeqLab) was used for cDNA synthesis using the RevertAid RT reverse transcription kit from Thermo Fisher Scientific. Transcript levels were measured based on SYBR Green technology using Promega GoTaq qPCR master mix according to the manufacturer's instructions. Data were analyzed using the $\Delta\Delta C_T$ method. Primers used for qPCR analyses are given in Supplemental Table 4.

Assessment of Photosynthesis and Transpiration Rates by Gas Exchange

Maximum photosynthesis rates were determined by CO_2 uptake (µmol CO_2 m^{-2} s^{-1}) measurements, and stomatal conductance was assessed via the determination of transpiration rates (mmol water m^{-2} s^{-1}) in intact leaves at a PPFD of 1000 µmol photons m^{-2} s^{-1} using a LI-6400XT portable photosynthesis system (LI-COR Environmental). Before recording the maximum photosynthetic rates, leaves were incubated for ~20 min in the measurement chamber until photosynthetic rates were stable. The temperature in the measuring cell was set to 22 to 23°C and the relative humidity was kept constant at 40% during measurements.

Reproducibility of Experiments and Statistical Analyses

The presented results are generally derived from one experimental data set, consisting of at least three biological replicates per treatment and genotype for metabolite and qPCR analyses, of seven biological replicates for bacterial growth assays, and of four biological replicates for IRGA analyses.

For qPCR analyses, values for biological replicates were calculated as the mean of two technical replicates. The presented results were similar in three independent experiments. For the statistical evaluation of the qPCR and metabolite data by Student's *t* test, $\log_{10}$-transformed relative expression and metabolite content values were analyzed. Bacterial growth data were analyzed by Student's *t* test without prior log transformation.

Assessment of the primed state was performed as described in Supplemental Figure 9 by comparing permutated differences of measured values by a two-sided Mann-Whitney U test (α = 0.005). To assess treatment effects, interaction terms between the two consecutive treatments, and between-experiment variation in the SAR-associated priming assays, the Pip-induced priming assays, and the Pip/SA coapplication assays, we assumed a linear model and performed ANOVA (Brady et al., 2015) with type II-sum of squares on Col-0 response data from three independent experiments using the R statistical package (https://www.r-project.org/) and the following command (see also Supplemental Tables 1 to 3):

$$\begin{aligned}\mathrm{ANOVA}(\mathrm{lm}(\mathrm{Phenotype}\sim&\mathrm{Treatment1}+\mathrm{Treatment2}+\mathrm{Experiment}\\&+\mathrm{Treatment1}*\mathrm{Treatment2}+\mathrm{Treatment1}*\mathrm{Experiment}\\&+\mathrm{Treatment2}*\mathrm{Experiment}+\mathrm{Treatment1}*\mathrm{Treatment2}\\&*\mathrm{Experiment},\ \mathrm{data}=\mathrm{object1}),\ \mathrm{type}=2).\end{aligned}$$

The statistical analysis of the RNA-seq data is described below.

Genome-Wide Transcriptional Analyses of the SAR State

Three biologically independent, replicate SAR induction experiments were performed as described in the paragraph above describing SAR experiments with Col-0 and *sid2* plants (experimental set 1) and three other biologically independent experiments with Col-0 and *ald1* plants (experimental set 2). In each SAR experiment, at least six upper (2°) leaves from six different plants pretreated in 1° leaves with *Psm* ($MgCl_2$) were pooled for one biological *Psm* (mock control) replicate. In this way, three biologically independent, replicate samples per treatment and plant genotype were obtained within each SAR set.

RNA was extracted from leaf sample replicates with the Plant RNeasy extraction kit (Qiagen) and treated on-column (Qiagen) and in solution with RNA-free DNase (New England Biolabs). RNA integrity, sequencing library quality, and fragment size were checked on a 2100 Bioanalyzer (Agilent). Libraries were prepared using the TruSeq RNA Sample Prep Kit v2 (Illumina), and library quantification was performed with a Qubit 2.0 (Invitrogen). Leaf samples were multiplexed 12 libraries per lane, yielding ~150 million reads per lane. All libraries were sequenced on the HiSeq 2500 Illumina platform. Libraries for the not stranded RNA-seq experiments were sequenced in the single end mode with length of 50 or 100 nucleotides.

Reads were demultiplexed and mapped to the *Arabidopsis* genome by the CLC bio Genomics Workbench with default parameters (alignment over at least 80% of the length of the read, up to three mismatches allowed) without alternative transcript detection. Differences in change ratios between mock and *Psm* treatment for the two independent Col-0 experimental sets were determined using a linear model framework [lm($\log_2$(rpm) ~ experiment*treatment)], resulting in no statistically different change ratios. The data for the two experimental sets were then combined for analyses. Differential expression between mock-treated and *Psm*-treated samples was calculated as a pairwise using edgeRs classic method on raw read counts as implemented in Bioconductor (Robinson et al., 2010). Genes are considered significantly differentially expressed if the FDR is below 0.01 (Benjamini and Hochberg, 1995). Reads per million (rpm) are reported for all transcripts. Reads per million were averaged for the replicates of each condition and the $\log_2$ of fold changes between *Psm* and mock values (=*P*/M-fold changes) were calculated by formally adding one read to all rpm values to account for transcripts with no expression detected in one or more samples before fold change calculation and logarithmic transformation (Bräutigam et al., 2011). This allowed us to keep genes with very low mock expression values but marked *Psm*-triggered expression in the data sets without significantly changing the actual logarithmized *P*/M ratios. Differences in change ratios between Col-0 and *sid2* for all genes without 0 counts in any experiment were determined using a linear model framework [lm($\log_2$(rpm) ~ genotype*treatment)] with P values corrected (Benjamini and Hochberg, 1995). The complete RNA-seq data of the SAR experiments are provided in Supplemental Data Set 1. Arabidopsis transcripts are annotated with descriptions from TAIR10 (Swarbreck et al., 2008) and functional annotations from MapMan (Thimm et al., 2004). Overlapping and exclusive membership in the significantly changed genes were calculated with Linux functions. To determine the percentages of SAR genes in specific gene categories or families (http://www.arabidopsis.org/), selected gene sets (major MapMan categories [Thimm et al., 2004], categories with a presumed role in defense signaling, and categories with an evident enrichment in SAR^+ and SAR^- genes based on careful inspection by eye of the whole data set) were aligned to the RNA-seq data set using the Excel macro FIRe (Garcion et al., 2006). Fisher's exact test ($P < 0.01$) corrected according to Benjamini and Hochberg (1995) was used to determine whether gene categories were significantly enriched or depleted in SAR^+ and SAR^- genes. GO term enrichment was analyzed and visualized using the GOrilla tool using the target and background gene list method (Eden et al., 2009).

Accession Numbers

RNA-seq data were deposited in the ArrayExpress database under the accession number E-MTAB-4151. Sequence data from this article can be found in the Arabidopsis Genome Initiative or GenBank/EMBL databases under the following accession numbers: *ALD1* (At2g13810), *FMO1* (At1g19250), *ICS1* (At1g74710), *PR-1* (At2g14610), *PAD4* (At3g52430), *NPR1* (At1g64280), *ARD3* (At2g26400), *SAG13* (At2g29350), and *GRXS13* (At1g03850).

Supplemental Data

Supplemental Figure 1. Identification of the *sid2 ald1* (*sid2-1 ald1*) double mutant.

Supplemental Figure 2. Characterization of the *sid2 ald1* double mutant.

Supplemental Figure 3. Systemic acquired resistance assay with Col-0 and *ics1 ics2* plants.

Supplemental Figure 4. Principle component analysis of the normalized transcriptome data.

Supplemental Figure 5. MapMan visualization: the transcriptional SAR response in Col-0.

Supplemental Figure 6. MapMan visualization: a diminished transcriptional SAR response exists in *sid2*.

Supplemental Figure 7. MapMan visualization: the transcriptional SAR response is absent in *ald1*.

Supplemental Figure 8. Percentage of SAR^+ and SAR^- genes in additional gene classes/families.

Supplemental Figure 9. SAR-associated defense priming: assay and definition.

Supplemental Figure 10. Graphs of Figure 6 with a linear scale for the *y* axes instead of a log scale.

Supplemental Figure 11. Graphs of Figure 7 with a linear scale for the *y* axes instead of a log scale.

Supplemental Figure 12. Graphs of Figure 8 with a linear scale for the *y* axes instead of a log scale.

Supplemental Figure 13. Pip-induced priming of salicylic acid biosynthesis requires functional *FMO1*.

Supplemental Figure 14. Graphs of Figures 9A and 9B with a linear scale for the *y* axes instead of a log scale.

Supplemental Figure 15. The transcriptional SAR response: activation of multiple stages of defense signaling.

Supplemental Table 1. Linear model-based analysis of the SAR-associated priming response in Col-0 plants to estimate treatment and experimental effect terms.

Supplemental Table 2. Linear model-based analysis of the pipecolic acid-induced priming response in Col-0 plants to estimate treatment and experimental effect terms.

Supplemental Table 3. Linear model-based analysis of the amplification of salicylic acid-induced *PR1* expression by pipecolic acid in Col-0 plants to estimate treatment and experimental effect terms.

Supplemental Table 4. List of primers used in this study.

Supplemental Data Set 1. Complete RNA-seq data of the SAR experiments with Col-0, *sid*2, and *ald1*.

Supplemental Data Set 2. GO term enrichment analysis of the SAR^- gene group.

Supplemental Data Set 3. GO term enrichment analysis of the SAR^+ gene group.

ACKNOWLEDGMENTS

This work was supported by the German Research Foundation (DFG Grant ZE467/6-1 and Graduate Program IRTG 1525). We thank Anna Busch for excellent technical assistance, Wolfgang Kaisers (Center for Bioinformatics and Biostatistics, HHU Düsseldorf), Markus Kollmann, and Martin Lercher for support on statistical issues and Jean-Pierre Métraux for kindly providing *ics1 ics2* seeds. We thank Michael Hartmann and Philippe Reymond for critically reading the manuscript.

AUTHOR CONTRIBUTIONS

F.B., A.-C.D., K.G., and S.S. performed the experiments. A.B., F.B., and J.Z. contributed to RNA-seq analyses and evaluation of expression data. F.B. and A.B. assisted J.Z. in manuscript preparation. J.Z. designed the research and wrote the manuscript.

Received June 5, 2015; revised November 30, 2015; accepted December 13, 2015; published December 15, 2015.

REFERENCES

Acharya, B.R., Raina, S., Maqbool, S.B., Jagadeeswaran, G., Mosher, S.L., Appel, H.M., Schultz, J.C., Klessig, D.F., and Raina, R. (2007). Overexpression of CRK13, an Arabidopsis cysteine-rich receptor-like kinase, results in enhanced resistance to *Pseudomonas syringae.* Plant J. **50:** 488–499.

Aliferis, K.A., Faubert, D., and Jabaji, S. (2014). A metabolic profiling strategy for the dissection of plant defense against fungal pathogens. PLoS One **9:** e111930.

Alonso, J.M., et al. (2003). Genome-wide insertional mutagenesis of *Arabidopsis thaliana.* Science **301:** 653–657.

Attaran, E., Zeier, T.E., Griebel, T., and Zeier, J. (2009). Methyl salicylate production and jasmonate signaling are not essential for systemic acquired resistance in Arabidopsis. Plant Cell **21:** 954–971.

Bartsch, M., Gobbato, E., Bednarek, P., Debey, S., Schultze, J.L., Bautor, J., and Parker, J.E. (2006). Salicylic acid-independent ENHANCED DISEASE SUSCEPTIBILITY1 signaling in Arabidopsis immunity and cell death is regulated by the monooxygenase FMO1 and the Nudix hydrolase NUDT7. Plant Cell **18:** 1038–1051.

Beckers, G.J., Jaskiewicz, M., Liu, Y., Underwood, W.R., He, S.Y., Zhang, S., and Conrath, U. (2009). Mitogen-activated protein kinases 3 and 6 are required for full priming of stress responses in *Arabidopsis thaliana.* Plant Cell **21:** 944–953.

Benjamini, Y., and Hochberg, Y. (1995). Controlling the false discovery rate: a practical and powerful approach to multiple testing. J. R. Stat. Soc. B **57:** 289–300.

Bisgrove, S.R., Simonich, M.T., Smith, N.M., Sattler, A., and Innes, R.W. (1994). A disease resistance gene in Arabidopsis with specificity for two different pathogen avirulence genes. Plant Cell **6:** 927–933.

Boller, T., and Felix, G. (2009). A renaissance of elicitors: perception of microbe-associated molecular patterns and danger signals by pattern-recognition receptors. Annu. Rev. Plant Biol. **60:** 379–406.

Bowling, S.A., Clarke, J.D., Liu, Y., Klessig, D.F., and Dong, X. (1997). The *cpr5* mutant of Arabidopsis expresses both NPR1-dependent and NPR1-independent resistance. Plant Cell **9:** 1573–1584.

Brady, S.M., Burow, M., Busch, W., Carlborg, Ö., Denby, K.J., Glazebrook, J., Hamilton, E.S., Harmer, S.L., Haswell, E.S., Maloof, J.N., Springer, N.M., and Kliebenstein, D.J. (2015). Reassess the t test: Interact with all your data via ANOVA. Plant Cell **27:** 2088–2094.

Bräutigam, A., et al. (2011). An mRNA blueprint for C4 photosynthesis derived from comparative transcriptomics of closely related C3 and C4 species. Plant Physiol. **155:** 142–156.

Breitenbach, H.H., et al. (2014). Contrasting roles of the apoplastic aspartyl protease APOPLASTIC, ENHANCED DISEASE SUSCEPTIBILITY1-DEPENDENT1 and LEGUME LECTIN-LIKE PROTEIN1 in Arabidopsis systemic acquired resistance. Plant Physiol. **165:** 791–809.

Broquist, H.P. (1991). Lysine-pipecolic acid metabolic relationships in microbes and mammals. Annu. Rev. Nutr. **11:** 435–448.

Bruce, T.J., Matthes, M.C., Napier, J.A., and Pickett, J.A. (2007). Stressful "memories" of plants: evidence for possible mechanisms. Plant Sci. **173:** 603–608.

Chaturvedi, R., Krothapalli, K., Makandar, R., Nandi, A., Sparks, A.A., Roth, M.R., Welti, R., and Shah, J. (2008). Plastid omega3-fatty acid desaturase-dependent accumulation of a systemic acquired resistance inducing activity in petiole exudates of *Arabidopsis thaliana* is independent of jasmonic acid. Plant J. **54:** 106–117.

Cheng, Y., Zhou, Y., Yang, Y., Chi, Y.J., Zhou, J., Chen, J.Y., Wang, F., Fan, B., Shi, K., Zhou, Y.H., Yu, J.Q., and Chen, Z. (2012). Structural and functional analysis of VQ motif-containing proteins in Arabidopsis as interacting proteins of WRKY transcription factors. Plant Physiol. **159:** 810–825.

Conrath, U. (2011). Molecular aspects of defence priming. Trends Plant Sci. **16:** 524–531.

Delaney, T.P., Friedrich, L., and Ryals, J.A. (1995). Arabidopsis signal transduction mutant defective in chemically and biologically induced disease resistance. Proc. Natl. Acad. Sci. USA **92:** 6602–6606.

Dempsey, D.A., and Klessig, D.F. (2012). SOS - too many signals for systemic acquired resistance? Trends Plant Sci. **17:** 538–545.

Derksen, H., Rampitsch, C., and Daayf, F. (2013). Signaling cross-talk in plant disease resistance. Plant Sci. **207:** 79–87.

Dey, S., et al. (2014). Bacteria-triggered systemic immunity in barley is associated with WRKY and ETHYLENE RESPONSIVE FACTORs but not with salicylic acid. Plant Physiol. **166:** 2133–2151.

Dubiella, U., Seybold, H., Durian, G., Komander, E., Lassig, R., Witte, C.P., Schulze, W.X., and Romeis, T. (2013). Calcium-dependent protein kinase/NADPH oxidase activation circuit is required for rapid defense signal propagation. Proc. Natl. Acad. Sci. USA **110:** 8744–8749.

Eden, E., Navon, R., Steinfeld, I., Lipson, D., and Yakhini, Z. (2009). GOrilla: a tool for discovery and visualization of enriched GO terms in ranked gene lists. BMC Bioinformatics **10:** 48.

Feys, B.J., Moisan, L.J., Newman, M.A., and Parker, J.E. (2001). Direct interaction between the Arabidopsis disease resistance signaling proteins, EDS1 and PAD4. EMBO J. **20:** 5400–5411.

Fritz-Laylin, L.K., Krishnamurthy, N., Tör, M., Sjölander, K.V., and Jones, J.D.G. (2005). Phylogenomic analysis of the receptor-like proteins of rice and Arabidopsis. Plant Physiol. **138:** 611–623.

Fu, Z.Q., Yan, S., Saleh, A., Wang, W., Ruble, J., Oka, N., Mohan, R., Spoel, S.H., Tada, Y., Zheng, N., and Dong, X. (2012). NPR3 and NPR4 are receptors for the immune signal salicylic acid in plants. Nature **486:** 228–232.

Fu, Z.Q., and Dong, X. (2013). Systemic acquired resistance: turning local infection into global defense. Annu. Rev. Plant Biol. **64:** 839–863.

Fujioka, S., and Sakurai, A. (1997). Conversion of lysine to L-pipecolic acid induces flowering in *Lemna paucicostata* 151. Plant Cell Physiol. **38:** 1278–1280.

Garcion, C., Baltensperger, R., Fournier, T., Pasquier, J., Schnetzer, M.A., Gabriel, J.P., and Métraux, J.-P. (2006). FiRe and microarrays: a fast answer to burning questions. Trends Plant Sci. **11:** 320–322.

Garcion, C., Lohmann, A., Lamodière, E., Catinot, J., Buchala, A., Doermann, P., and Métraux, J.P. (2008). Characterization and biological function of the ISOCHORISMATE SYNTHASE2 gene of Arabidopsis. Plant Physiol. **147:** 1279–1287.

Goda, H., et al. (2008). The AtGenExpress hormone and chemical treatment data set: experimental design, data evaluation, model data analysis and data access. Plant J. **55:** 526–542.

Gruner, K., Griebel, T., Návarová, H., Attaran, E., and Zeier, J. (2013). Reprogramming of plants during systemic acquired resistance. Front. Plant Sci. **4:** 252.

Gupta, R.N., and Spenser, I.D. (1969). Biosynthesis of the piperidine nucleus. The mode of incorporation of lysine into pipecolic acid and into piperidine alkaloids. J. Biol. Chem. **244:** 88–94.

Hilfiker, O., Groux, R., Bruessow, F., Kiefer, K., Zeier, J., and Reymond, P. (2014). Insect eggs induce a systemic acquired resistance in Arabidopsis. Plant J. **80:** 1085–1094.

Jing, B., Xu, S., Xu, M., Li, Y., Li, S., Ding, J., and Zhang, Y. (2011). Brush and spray: a high-throughput systemic acquired resistance assay suitable for large-scale genetic screening. Plant Physiol. **157:** 973–980.

Jirage, D., Tootle, T.L., Reuber, T.L., Frost, L.N., Feys, B.J., Parker, J.E., Ausubel, F.M., and Glazebrook, J. (1999). *Arabidopsis thaliana PAD4* encodes a lipase-like gene that is important for salicylic acid signaling. Proc. Natl. Acad. Sci. USA **96:** 13583–13588.

Jung, H.W., Tschaplinski, T.J., Wang, L., Glazebrook, J., and Greenberg, J.T. (2009). Priming in systemic plant immunity. Science **324:** 89–91.

Kauss, H., Theisinger-Hinkel, E., Mindermann, R., and Conrath, U. (1992). Dichloroisonicotinic and salicylic acid, inducers of systemic acquired resistance, enhance fungal elicitor responses in parsley cells. Plant J. **2:** 655–660.

Kim, T.H., Kunz, H.H., Bhattacharjee, S., Hauser, F., Park, J., Engineer, C., Liu, A., Ha, T., Parker, J.E., Gassmann, W., and Schroeder, J.I. (2012). Natural variation in small molecule-induced TIR-NB-LRR signaling induces root growth arrest via EDS1- and PAD4-complexed R protein VICTR in Arabidopsis. Plant Cell **24:** 5177–5192.

Koch, M., Vorwerk, S., Masur, C., Sharifi-Sirchi, G., Olivieri, N., and Schlaich, N.L. (2006). A role for a flavin-containing mono-oxygenase in resistance against microbial pathogens in Arabidopsis. Plant J. **47:** 629–639.

Kohler, A., Schwindling, S., and Conrath, U. (2002). Benzothiadiazole-induced priming for potentiated responses to pathogen infection, wounding, and infiltration of water into leaves requires the *NPR1/NIM1* gene in Arabidopsis. Plant Physiol. **128:** 1046–1056.

Koornneef, A., and Pieterse, C.M.J. (2008). Cross talk in defense signaling. Plant Physiol. **146:** 839–844.

La Camera, S., L'haridon, F., Astier, J., Zander, M., Abou-Mansour, E., Page, G., Thurow, C., Wendehenne, D., Gatz, C., Métraux, J.-P., and Lamotte, O. (2011). The glutaredoxin ATGRXS13 is required to facilitate *Botrytis cinerea* infection of *Arabidopsis thaliana* plants. Plant J. **68:** 507–519.

Masclaux-Daubresse, C., Clément, G., Anne, P., Routaboul, J.M., Guiboileau, A., Soulay, F., Shirasu, K., and Yoshimoto, K. (2014). Stitching together the multiple dimensions of autophagy using metabolomics and transcriptomics reveals impacts on metabolism, development, and plant responses to the environment in Arabidopsis. Plant Cell **26:** 1857–1877.

Mateo, A., Funck, D., Mühlenbock, P., Kular, B., Mullineaux, P.M., and Karpinski, S. (2006). Controlled levels of salicylic acid are required for optimal photosynthesis and redox homeostasis. J. Exp. Bot. **57:** 1795–1807.

Mauch, F., Mauch-Mani, B., Gaille, C., Kull, B., Haas, D., and Reimmann, C. (2001). Manipulation of salicylate content in *Arabidopsis thaliana* by the expression of an engineered bacterial salicylate synthase. Plant J. **25:** 67–77.

Melotto, M., Underwood, W., Koczan, J., Nomura, K., and He, S.Y. (2006). Plant stomata function in innate immunity against bacterial invasion. Cell **126:** 969–980.

Memelink, J. (2009). Regulation of gene expression by jasmonate hormones. Phytochemistry **70:** 1560–1570.

Mishina, T.E., Griebel, T., Geuecke, M., Attaran, E., and Zeier, J. (2008). New insights into the molecular events underlying systemic acquired resistance. In Biology of Plant-Microbe Interactions, Vol. 6, M. Lorito, S.L. Woo, and F. Scala, eds (St. Paul, MN: International Society for Molecular Plant-Microbe Interactions), paper 81.

Mishina, T.E., and Zeier, J. (2006). The Arabidopsis flavin-dependent monooxygenase FMO1 is an essential component of biologically induced systemic acquired resistance. Plant Physiol. **141:** 1666–1675.

Mishina, T.E., and Zeier, J. (2007). Pathogen-associated molecular pattern recognition rather than development of tissue necrosis contributes to bacterial induction of systemic acquired resistance in Arabidopsis. Plant J. **50:** 500–513.

Mölders, W., Buchala, A., and Métraux, J.-P. (1996). Transport of salicylic acid in tobacco necrosis virus-infected cucumber plants. Plant Physiol. **112:** 787–792.

Moore, J.W., Loake, G.J., and Spoel, S.H. (2011). Transcription dynamics in plant immunity. Plant Cell **23:** 2809–2820.

Morrison, R.I. (1953). The isolation of L-pipecolinic acid from *Trifolium repens*. Biochem. J. **53:** 474–478.

Mur, L.A.J., Grant, N., Warner, S.A.J., Sugars, J.M., White, R.F., and Draper, J. (1996). Salicylic acid potentiates defence gene expression in tissue exhibiting acquired resistance to pathogen attack. Plant J. **9:** 550–571.

Návarová, H., Bernsdorff, F., Döring, A.-C., and Zeier, J. (2012). Pipecolic acid, an endogenous mediator of defense amplification and priming, is a critical regulator of inducible plant immunity. Plant Cell **24:** 5123–5141.

Nawrath, C., and Métraux, J.-P. (1999). Salicylic acid induction-deficient mutants of Arabidopsis express *PR-2* and *PR-5* and

accumulate high levels of camalexin after pathogen inoculation. Plant Cell **11:** 1393–1404.

Noutoshi, Y., Okazaki, M., Kida, T., Nishina, Y., Morishita, Y., Ogawa, T., Suzuki, H., Shibata, D., Jikumaru, Y., Hanada, A., Kamiya, Y., and Shirasu, K. (2012). Novel plant immune-priming compounds identified via high-throughput chemical screening target salicylic acid glucosyltransferases in Arabidopsis. Plant Cell **24:** 3795–3804.

Pálfi, G., and Dézsi, L. (1968). Pipecolic acid as an indicator of abnormal protein metabolism in diseased plants. Plant Soil **29:** 285–291.

Pandey, S.P., and Somssich, I.E. (2009). The role of WRKY transcription factors in plant immunity. Plant Physiol. **150:** 1648–1655.

Rietz, S., Stamm, A., Malonek, S., Wagner, S., Becker, D., Medina-Escobar, N., Vlot, A.C., Feys, B.J., Niefind, K., and Parker, J.E. (2011). Different roles of Enhanced Disease Susceptibility1 (EDS1) bound to and dissociated from Phytoalexin Deficient4 (PAD4) in Arabidopsis immunity. New Phytol. **191:** 107–119.

Robinson, M.D., McCarthy, D.J., and Smyth, G.K. (2010). edgeR: a Bioconductor package for differential expression analysis of digital gene expression data. Bioinformatics **26:** 139–140.

Sauter, M., Lorbiecke, R., Ouyang, B., Pochapsky, T.C., and Rzewuski, G. (2005). The immediate-early ethylene response gene OsARD1 encodes an acireductone dioxygenase involved in recycling of the ethylene precursor S-adenosylmethionine. Plant J. **44:** 718–729.

Schenk, S.T., Hernández-Reyes, C., Samans, B., Stein, E., Neumann, C., Schikora, M., Reichelt, M., Mithöfer, A., Becker, A., Kogel, K.H., and Schikora, A. (2014). N-acyl-homoserine lactone primes plants for cell wall reinforcement and induces resistance to bacterial pathogens via the salicylic acid/oxylipin pathway. Plant Cell **26:** 2708–2723.

Schlaich, N.L. (2007). Flavin-containing monooxygenases in plants: looking beyond detox. Trends Plant Sci. **12:** 412–418.

Serrano, M., Wang, B., Aryal, B., Garcion, C., Abou-Mansour, E., Heck, S., Geisler, M., Mauch, F., Nawrath, C., and Métraux, J.-P. (2013). Export of salicylic acid from the chloroplast requires the multidrug and toxin extrusion-like transporter EDS5. Plant Physiol. **162:** 1815–1821.

Shah, J., and Zeier, J. (2013). Long-distance communication and signal amplification in systemic acquired resistance. Front. Plant Sci. **4:** 30.

Shiu, S.H., and Bleecker, A.B. (2001). Receptor-like kinases from Arabidopsis form a monophyletic gene family related to animal receptor kinases. Proc. Natl. Acad. Sci. USA **98:** 10763–10768.

Shulaev, V., Leon, J., and Raskin, I. (1995). Is salicylic acid a translocated signal of systemic acquired resistance in tobacco? Plant Cell **7:** 1691–1701.

Singh, P., Yekondi, S., Chen, P.W., Tsai, C.H., Yu, C.W., Wu, K., and Zimmerli, L. (2014). Environmental history modulates Arabidopsis pattern-triggered immunity in a HISTONE ACETYLTRANSFERASE1-dependent manner. Plant Cell **26:** 2676–2688.

Song, J.T., Lu, H., and Greenberg, J.T. (2004a). Divergent roles in Arabidopsis thaliana development and defense of two homologous genes, aberrant growth and death2 and AGD2-LIKE DEFENSE RESPONSE PROTEIN1, encoding novel aminotransferases. Plant Cell **16:** 353–366.

Song, J.T., Lu, H., McDowell, J.M., and Greenberg, J.T. (2004b). A key role for ALD1 in activation of local and systemic defenses in Arabidopsis. Plant J. **40:** 200–212.

Sticher, L., Mauch-Mani, B., and Métraux, J.P. (1997). Systemic acquired resistance. Annu. Rev. Phytopathol. **35:** 235–270.

Swarbreck, D., et al. (2008). The Arabidopsis Information Resource (TAIR): gene structure and function annotation. Nucleic Acids Res. **36:** D1009–D1014.

Tan, X., Meyers, B.C., Kozik, A., West, M.A., Morgante, M., St Clair, D.A., Bent, A.F., and Michelmore, R.W. (2007). Global expression analysis of nucleotide binding site-leucine rich repeat-encoding and related genes in Arabidopsis. BMC Plant Biol. **7:** 56.

Tateda, C., Zhang, Z., Shrestha, J., Jelenska, J., Chinchilla, D., and Greenberg, J.T. (2014). Salicylic acid regulates Arabidopsis microbial pattern receptor kinase levels and signaling. Plant Cell **26:** 4171–4187.

Thibaud-Nissen, F., Wu, H., Richmond, T., Redman, J.C., Johnson, C., Green, R., Arias, J., and Town, C.D. (2006). Development of Arabidopsis whole-genome microarrays and their application to the discovery of binding sites for the TGA2 transcription factor in salicylic acid-treated plants. Plant J. **47:** 152–162.

Thimm, O., Bläsing, O., Gibon, Y., Nagel, A., Meyer, S., Krüger, P., Selbig, J., Müller, L.A., Rhee, S.Y., and Stitt, M. (2004). MAPMAN: a user-driven tool to display genomics data sets onto diagrams of metabolic pathways and other biological processes. Plant J. **37:** 914–939.

Thulke, O., and Conrath, U. (1998). Salicylic acid has a dual role in the activation of defence-related genes in parsley. Plant J. **14:** 35–42.

Truman, W., Bennett, M.H., Kubigsteltig, I., Turnbull, C., and Grant, M. (2007). Arabidopsis systemic immunity uses conserved defense signaling pathways and is mediated by jasmonates. Proc. Natl. Acad. Sci. USA **104:** 1075–1080.

Tsuda, K., Mine, A., Bethke, G., Igarashi, D., Botanga, C.J., Tsuda, Y., Glazebrook, J., Sato, M., and Katagiri, F. (2013). Dual regulation of gene expression mediated by extended MAPK activation and salicylic acid contributes to robust innate immunity in *Arabidopsis thaliana*. PLoS Genet. **9:** e1004015.

Vernooij, B., Friedrich, L., Morse, A., Reist, R., Kolditz-Jawhar, R., Ward, E., Uknes, S., Kessmann, H., and Ryals, J. (1994). Salicylic acid is not the translocated signal responsible for inducing systemic acquired resistance but is required in signal transduction. Plant Cell **6:** 959–965.

Vivancos, J., Labbé, C., Menzies, J.G., and Bélanger, R.R. (2015). Silicon-mediated resistance of Arabidopsis against powdery mildew involves mechanisms other than the salicylic acid (SA)-dependent defence pathway. Mol. Plant Pathol. **16:** 572–582.

Vlot, A.C., Dempsey, D.A., and Klessig, D.F. (2009). Salicylic acid, a multifaceted hormone to combat disease. Annu. Rev. Phytopathol. **47:** 177–206.

Vogel-Adghough, D., Stahl, E., Návarová, H., and Zeier, J. (2013). Pipecolic acid enhances resistance to bacterial infection and primes salicylic acid and nicotine accumulation in tobacco. Plant Signal. Behav. **8:** e26366.

von Caemmerer, S., and Farquhar, G.D. (1981). Some relationships between the biochemistry of photosynthesis and the gas exchange of leaves. Planta **153:** 376–387.

Wang, D., Amornsiripanitch, N., and Dong, X. (2006). A genomic approach to identify regulatory nodes in the transcriptional network of systemic acquired resistance in plants. PLoS Pathog. **2:** e123.

Ward, E.R., Uknes, S.J., Williams, S.C., Dincher, S.S., Wiederhold, D.L., Alexander, D.C., Ahl-Goy, P., Métraux, J.P., and Ryals, J.A. (1991). Coordinate gene activity in response to agents that induce systemic acquired resistance. Plant Cell **3:** 1085–1094.

Wildermuth, M.C., Dewdney, J., Wu, G., and Ausubel, F.M. (2001). Isochorismate synthase is required to synthesize salicylic acid for plant defence. Nature **414:** 562–565.

Wu, Y., Zhang, D., Chu, J.Y., Boyle, P., Wang, Y., Brindle, I.D., De Luca, V., and Després, C. (2012). The *Arabidopsis* NPR1 protein is a receptor for the plant defense hormone salicylic acid. Cell Reports **1:** 639–647.

Yan, H., Yoo, M.J., Koh, J., Liu, L., Chen, Y., Acikgoz, D., Wang, Q., and Chen, S. (2014). Molecular reprogramming of Arabidopsis in response to perturbation of jasmonate signaling. J. Proteome Res. **13:** 5751–5766.

Zacharius, R.M., Thompson, J.F., and Steward, F.C. (1954). The detection, isolation and identification of L(-)-pipecolic acid in the non-protein fraction of beans (*Phaseolus vulgaris*). J. Am. Chem. Soc. **76:** 2908–2912.

Zander, M., Thurow, C., and Gatz, C. (2014). TGA transcription factors activate the salicylic acid-suppressible branch of the ethylene-induced defense program by regulating ORA59 expression. Plant Physiol. **165:** 1671–1683.

Zeier, J. (2013). New insights into the regulation of plant immunity by amino acid metabolic pathways. Plant Cell Environ. **36:** 2085–2103.

Zeier, J., Pink, B., Mueller, M.J., and Berger, S. (2004). Light conditions influence specific defence responses in incompatible plant-pathogen interactions: uncoupling systemic resistance from salicylic acid and PR-1 accumulation. Planta **219:** 673–683.

Zeng, W., Brutus, A., Kremer, J.M., Withers, J.C., Gao, X., Jones, A.D., and He, S.Y. (2011). A genetic screen reveals Arabidopsis stomatal and/or apoplastic defenses against *Pseudomonas syringae* pv. *tomato* DC3000. PLoS Pathog. **7:** e1002291.

Zhou, N., Tootle, T.L., Tsui, F., Klessig, D.F., and Glazebrook, J. (1998). PAD4 functions upstream from salicylic acid to control defense responses in Arabidopsis. Plant Cell **10:** 1021–1030.

Zimmerli, L., Jakab, G., Métraux, J.-P., and Mauch-Mani, B. (2000). Potentiation of pathogen-specific defense mechanisms in Arabidopsis by β -aminobutyric acid. Proc. Natl. Acad. Sci. USA **97:** 12920–12925.

Zipfel, C. (2014). Plant pattern-recognition receptors. Trends Immunol. **35:** 345–351.

Zoeller, M., Stingl, N., Krischke, M., Fekete, A., Waller, F., Berger, S., and Mueller, M.J. (2012). Lipid profiling of the Arabidopsis hypersensitive response reveals specific lipid peroxidation and fragmentation processes: biogenesis of pimelic and azelaic acid. Plant Physiol. **160:** 365–378.